PSSD EUROPE
Power Systems Design: Empowering Global Innovation
July/August 2013

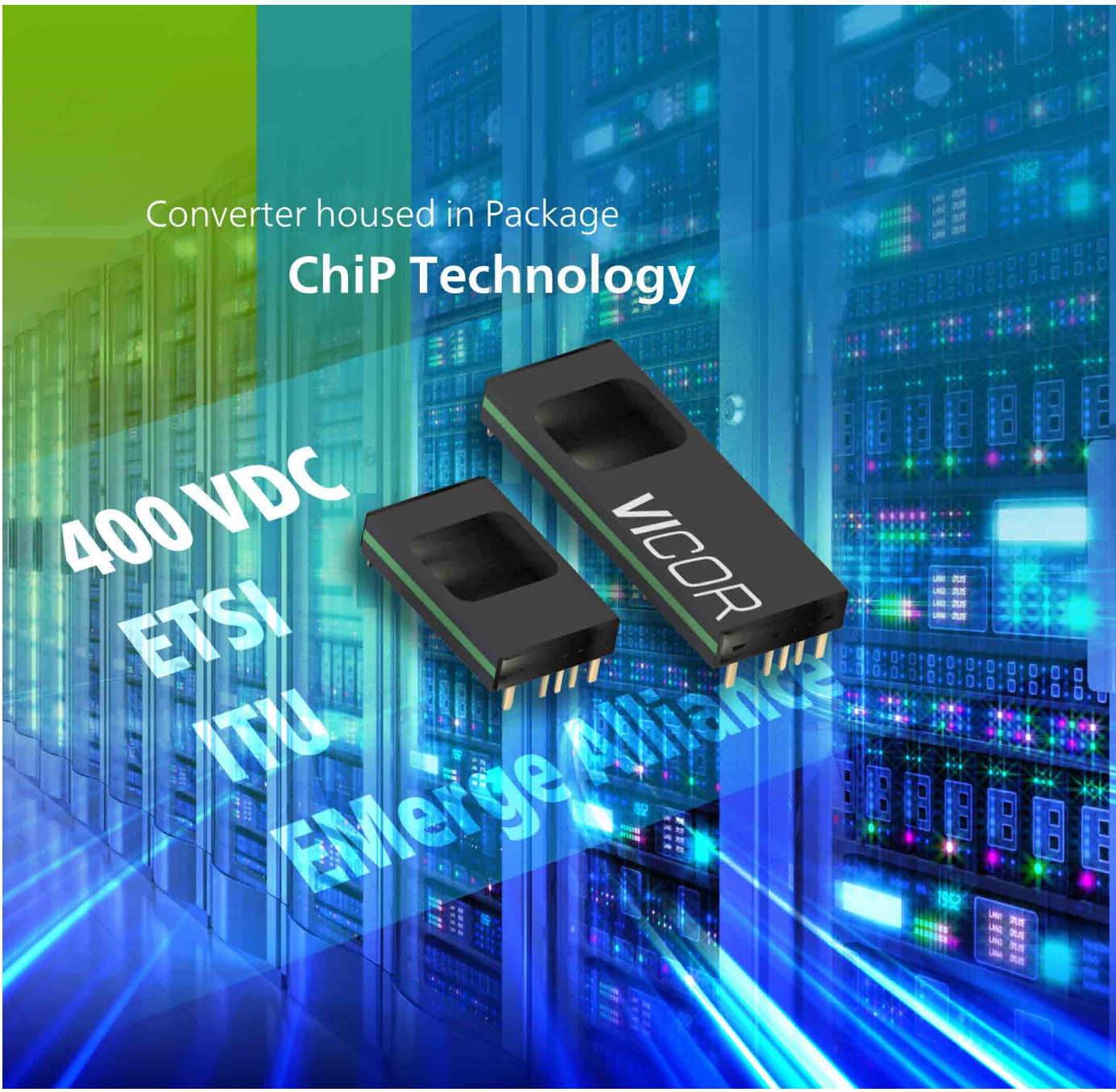

Special Report: Automotive (pg 33)

PSD EUROPE

Power Systems Design: Empowering Global Innovation

WWW.POWERSYSTEMSDESIGN.COM

Visit us online for exclusive content; Industry News, Products, Reviews, and full PSD archives and back issues

COVER STORY

Addressing 400-Vdc power in advanced industrial and data-center apps (pg 14)

Highlighted Products News, Industry News and more web-only content, to:

www.powersystemsdesign.com

PSD EUROPE

AGS Media Group
146 Charles Street
Annapolis, MD 21401 USA
Tel: +410.295.0177
Fax: +510.217.3608
www.powersystemsdesign.com

Editorial Director
Alix Paultre, Editorial Director,
Power Systems Design
alixp@powersystemsdesign.com

Contributing Editors
Liu Hong, Editor-in-Chief,
Power Systems Design China
powersdc@126.com

Ryan Sanderson, IMS Research
ryan.sanderson@imsresearch.com

Dr. Ray Ridley, Ridley Engineering
RRidley@ridleyengineerng.com

Publishing Director
Jim Graham
jim.graham@powersystemsdesign.com

Publisher
Julia Stocks
Julia.stocks@powersystemsdesign.com

Production Manager
Chris Corneal
chris.corneal@powersystemsdesign.com

Circulation Management
Christie Penque
christie.penque@powersystemsdesign.com

Magazine Design
Louis C. Geiger
louis@agencyofrecord.com

Registration of copyright: January 2004
ISSN number: 1613-6365

Volume 10, Issue 6

Today's cutting-edge creators

America has a legacy of basement and backyard tinkers inventing (or developing) often-revolutionary technologies in every application space in existence (and for some that never appeared). Creating things is in our bones, and the latest crop of scrappy inventors creating new applications for the latest state of the art embedded systems is doing some amazing things.

A great deal of this development comes from the artistic community. Musicians, artists, dancers, and other performance artists are incorporating sophisticated electronic embedded systems into their performances, creating new application spaces and marketplaces for the electronics industry.

The flattened Earth of open technology enablement has significantly reduced the organizational resources required as well as eased access to a worldwide base of materials, talent, and information (the most powerful part of the equation today).

In addition, baseline quality of manufacturing has gone up. Any good CNC machine will give you tolerances that would have given tool shops fits a couple of decades ago. Technologies like additive manufacturing (3D printing) have broken down the barriers between concept and creation.

It has gotten to the point that most audiences are used to seeing integrated video and images in entertainment. The latest example can be found in the "3D video mapping" dance group called "Sensation" currently competing on the show "America's got Talent". Video mapping is the practice of projecting images onto (often unconventional) surfaces, and this group uses large (roughly a meter or so) cubes with internal projectors showing various images and videos they dance in harmony with.

The dancers are really dancing on the tip of a technological iceberg they do not perceive because it is mostly under the waterline. Someone made the projectors and designed the light engines and optics to operate properly while being bounced around by a bunch of people; someone designed the interface that allows the director to control and program the images; someone designed the battery-based power system (with the same strictures on bouncy integrity) that allowed the group to throw the things around while operating in the first place.

This is related to the "Maker Revolution", in that anybody who so desires can create a pretty complex system now from building-block subsystems and advanced development technologies readily available. This obviously goes beyond dancers, has already impacted application spaces from consumer to aerospace.

This does not have to bypass the old guard; in fact this leveling of the playing field most benefits those with experience and knowledge in their industry, as they can now actualize their ideas to create value within their market by harnessing these new tools and processes to achieve their goals.

Best Regards,

Alix Paultre

Editorial Director, Power Systems Design
alixp@powersystemsdesign.com

Ultra-compact high-efficiency supplies address automotive applications

In recent years the increasing popularity of electric and hybrid vehicles has led to more sophisticated electronic systems and a greater demand for microcontrollers and memory. Conventional LDO regulators are commonly used, but they feature poor efficiency and cannot meet higher current demands. As a result, DC/DC converters, which provide greater efficiency and higher current-handling capability, are becoming the preferred solution. However, they are not without their drawbacks, which include more external parts and consequently a larger mounting area, increasing circuit design complexity significantly. With the trend towards improved performance and decreasing model cycles in the automotive industry comes a need for easier-to-use, high efficiency power supply ICs that lighten the design load and minimize mounting area.

A primary factor in the number of external components used with power supply ICs is the phase compensation circuit required to maintain a stable output voltage. Normally external capacitors and resistors are used to set the desired characteristics. However, ROHM was able to successfully optimize the phase compensation circuit internally, reducing parts count by 80% and contributing to more compact automotive systems. In addition, phase compensation adjustment, which is a common problem with power supply designs, is no longer required, shortening design time significantly. The power supplies use synchronous rectification for high efficiency operation, in combination with Light Load Mode, ensuring superior performance with low current consumption under all load conditions.

Key Features

Built-in phase compensation circuit and feedback resistors

The BD905xx series integrates an optimized phase compensation circuit that reduces the number of external components considerably, simplifying set design while minimizing mounting area.

Compact package

The HTSOP-J8 package reduces volume by approx. 80% compared with conventional products. (6.0mmx4.9mm, t=1.0mm max.)

Low heat generation simplifies thermal design

Loss is 1/10th that of conventional LDO regulators, resulting in minimal heat generation. This simplifies thermal countermeasures, making it ideal for microcontrollers and DDR memory used in today's vehicles that require greater current consumption.

Synchronous rectification and Light Load Mode

Synchronous rectification, coupled with Light Load Mode, results in over 90% efficiency (max.) under all load conditions for minimal current consumption.

ROHM Semiconductor (www.rohm.com/eu)

Joint laboratory effort to drive the development of next-gen vehicles

By: Marco Monti, STMicroelectronics

STMicroelectronics, a global semiconductor leader serving customers across the spectrum of electronics applications and a leading supplier of automotive electronics, together with Great Wall Motor Company Limited (GWM), China's leading SUV and pickup manufacturer and privately owned enterprise, announced a strategic partnership and the establishment of a joint development laboratory at GWM's Technical Center. The joint lab will focus on advanced research and development of cutting-edge solutions in powertrain, chassis, safety, car body, car infotainment, as well as new-energy technologies and other automotive applications.

ST will contribute its newest automotive-electronics technologies and solutions including GDI (Gasoline Direct Injection) and BCM (Body Control Modules), automotive-class devices such as the PowerPC™ series 32-bit microcontrollers, highly integrated solutions for EMS (Engine Management System) and Safety (Passive and Active), complete platforms for Infotainment (Audio, Video, Connectivity, and Navigation) , reference designs, development tools, technical support and trainings for many different automotive applications.

"The automotive electronics market is seeing rapid growth. Confronted with unprecedented competitive pressure, local automotive companies must implement strategic transformation and develop their own core technologies to compete with joint-venture brands. With consumers paying more attention to safety and comfort in the car, those are among the areas in which we can add great value," said Mr. Huang Yong, Senior Vice President and Chief Director of Technical Center, Great Wall Motor. "The establishment of a joint laboratory with ST will play a very important role in helping GWM to enhance our core competences in automotive electronics and it will build a solid foundation for deep cooperation of both parties in the future."

We are honored to cooperate with Great Wall, one of the most innovative and fastest growing car makers in China. The market and the consumers are increasingly asking for better fuel efficiency, safety, comfort and infotainment, and we are bringing all the right ingredients to this co-operation: leading-edge technologies and products, expertise, and total commitment to Automotive. The cooperation of Great Wall and ST is well positioned to address and anticipate the requirements and new directions in automotive electronics applications."

Great Wall Motor Company is a leading Chinese SUV and pickup manufacturer and privately owned enterprise, has over 50 holding subsidiaries with more than 56,000 employees. STMicroelectronics is a leader in the semiconductor market serving customers across the spectrum of sense and power and automotive products and embedded processing solutions.

www.st.com

Road Electrification provides opportunities for battery management

By: Ryan Sanderson, IHS

Simple battery management systems (BMS) are used extensively in consumer electronics and usually consist of one or more battery management ICs to control charging, perform authentication, provide protection, measure the state of charge, and balance the cells. As battery chemistry changes and the number of cells increases, although the fundamental design of a BMS remains the same, its complexity increases. For example, in hybrid electric vehicles (HEV), plug-in hybrid electric vehicles (PHEV) and battery electric vehicles (BEV), there are hundreds of times more cells than in consumer electronics. Although this poses challenges, it also provides opportunities. The market for automotive and motive batteries is projected to grow by $16 billion from 2013 to 2017. Unit shipments are predicted to grow by 27% during this period.

Although a BMS can be designed for use with any battery chemistry, in the automotive/motive market, most are designed for lithium-ion batteries. For lithium-ion batteries, the BMS is crucial as lithium is inherently unstable. Sensitivity to high temperature can result in degradation of the battery pack; and reported instances of thermal runaway resulting in lithium-ion batteries catching fire have led to concerns regarding safety. That being said, properly managed, lithium-ion batteries are a perfectly viable solution for vehicle propulsion and growth in this market is forecast to accelerate rapidly over the next five years.

Recent findings from the IHS report "The World Market for Motive Batteries" revealed that lithium-ion batteries were installed in 8% of HEVs in 2012, driving a market worth $113 million. By 2017, it is predicted that 48% of HEVs will have lithium-ion batteries installed and that the market will be worth $735 million. This excludes any battery management, though each battery pack will require at least one BMS.

Similarly, unit shipments of battery packs (excluding BMS) for PHEVs are projected to increase by a factor of ten from 70,000 in 2012 to 700,000 in 2017. The market for lithium-ion batteries in BEVs is more established and was estimated to be worth $1.2 billion in 2012. This is also projected to grow rapidly, more than tripling from 2012 to 2017. A further $500 million of growth in sales of lithium-ion batteries during this period is forecast to be driven by the rapidly increasing demand for electric bikes in Europe and America (in Asia, the majority of these bikes use low-cost lead-acid batteries).

In total, the electric road vehicle sector is predicted to drive shipments of lithium-ion batteries from 1.7 million in 2012 to 6.3 million in 2017. This will offer huge opportunities for battery packers, BMS manufacturers and semiconductor manufacturers. And this is just one part of the total motive/automotive battery market. Demand for greater accuracy and charge monitoring is also driving demand for BMS in applications that use other battery types, such as lead-acid and nickel metal-hydride. This will bring further opportunities in what is proving to be a dynamic and fast-paced market.

www.ihs.com

PWM Switch Modeling

By: Dr. Ray Ridley, President, Ridley Engineering

Soon after switching power supplies were implemented in industry in the 60s and 70s, it became apparent that they had unique issues with control that defied normal circuit analysis. This gave rise to state-space averaging, a technique with which the two distinct conditions of the power switch and diode could be combined and analyzed for the first time.

State-space averaging was a powerful analytical tool that enabled development of control systems for many years. However, it was mathematically cumbersome and difficult for newcomers to the field of power electronics to grasp intuitively.

Dr. Vatché Vorpérian developed the PWM switch model in 1986, which replaced the need for state-space averaging and simplified the analysis process. It was a very elegant and intuitive modeling approach, which is easily grasped by new students in the field. Twenty-seven years later, it is still the most accurate and useful way to analyze your circuit.

In this article, we look at the PWM

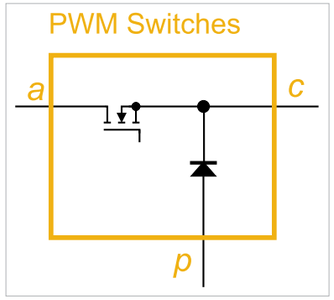

Figure 1: PWM switches needed to create a switching power supply. The diode can also be a synchronous rectifier if desired.

switch elements, and the three forms of the equivalent circuit model which can be used for different types of analysis.

PWM Switch Model

Figure 1 shows the essential switching elements of a power supply. There must always be a controlled switch, and a diode (or second switch) that is on when the controlled switch is off. The junction of the two elements is connected to a common terminal, which will be connected to any inductors in the switching power stage.

Vorpérian showed that there are three equivalent circuits that can replace the actual switching elements to perform

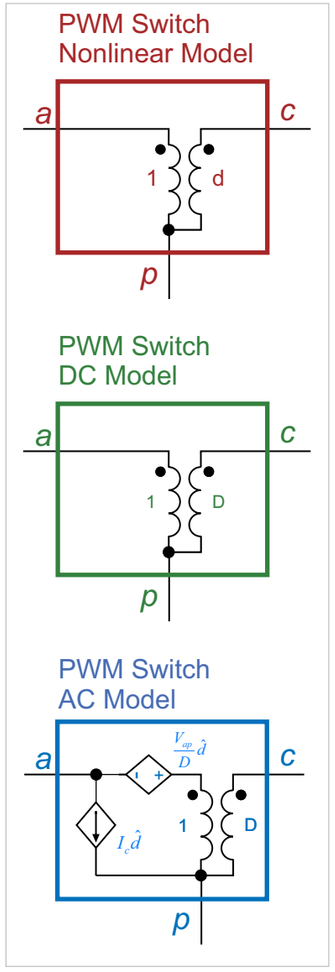

Figure 2: Three different equivalent circuits – the nonlinear switch model, linearized small-signal switch model, and DC switch model.

different levels of circuit analysis. The first of these, shown in **Figure 2** with red components, enables you to analyze a circuit for nonlinear effects. This equivalent circuit consists of a 1:d transformer. The value of the turns ratio, d, is set by the output of the controller for the power supply, and is a continuously variable function with a value between 0 and 1. Switching is eliminated in this circuit.

This circuit can be used by an analysis program such as Spice to predict waveforms and small-signal analysis, but the nonlinear operation of such an element can cause Spice to have numerical convergence issues under some circumstances.

Linearization is needed if we are to perform manual analysis on a switched-mode power supply to derive symbolic results rather than numerical results. The blue circuit of Figure 2 shows the linearized model which is the one that is most frequently used in the power electronics industry. This equivalent circuit has two additional sources added. Also, a 1:D transformer is added where

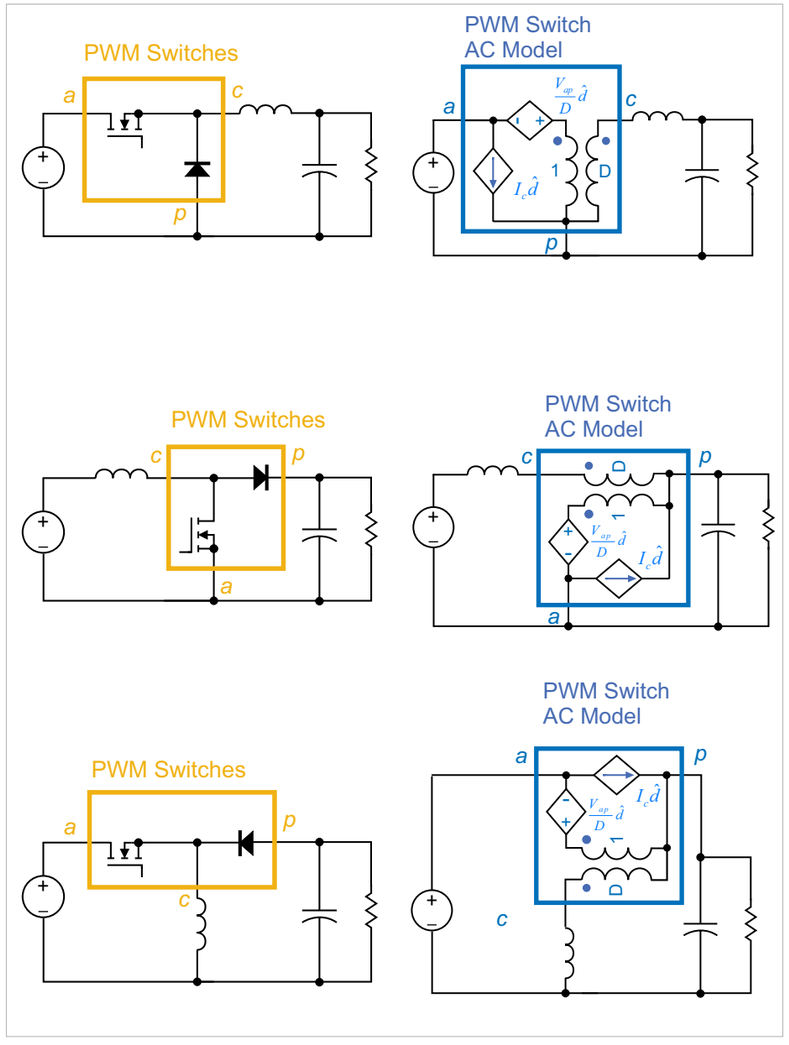

Figure 3: Linearized small-signal switch model inserted into the buck, boost, and buck-boost converters. A single Spice subcircuit suffices for all converters.

D is the steady-state duty cycle, which defines the operating point of the circuit.

If there is no perturbation of duty cycle and you just want to find the DC gain of a power stage, you can use the green circuit of Figure 2. This retains only the 1:D transformer from the complete AC circuit model shown in blue. This circuit can also be used to find transfer functions that do not involve perturbation of the duty cycle, such as the open-loop output impedance.

PWM Switch Model in Different Converters

The major challenge to implementing the PWM switch model is finding the switch and diode combination arranged appropriately in your particular power circuit. This is trivial for the three fundamental circuits—the buck, boost, and buck-boost, as discussed in [1]. As shown in **Figure 3**, the switch and diode of these circuits naturally appear next to each other. Replacement of the switching elements with

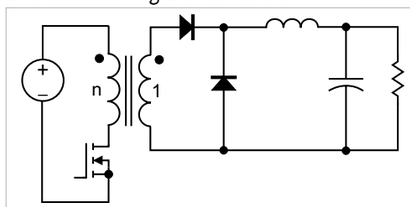

Figure 4: Rearrangement of the forward converter components reveals the PWM switching components, leading to the small-signal model which includes a transformer.

the small-signal equivalent circuit is then straightforward.

Notice that all three of the basic circuits have the same model for the PWM switch subcircuit. However, the converters have very different characteristics—a moving double pole and RHP zeros for the boost and buck-boost. These unusual characteristics are created because of the rotation of the PWM switch, and its insertion between the inductor and capacitor.

When a transformer is used as part of the power stage, the switch and diode can be separated. A little more work is needed on the circuit to identify the PWM switch model. An example of this is shown in **Figure 4**. For a single-switch forward converter, the switch is on the primary of the transformer, and the diode is on the secondary.

A simple circuit transformation pushes the switch through to the secondary side, where it appears in series with the forward diode. Notice this circuit has a voltage source now connected across an ideal transformer. (We could not implement an ideal transformer in real life, but it is not a problem conceptually, or for Spice to model.) The current in the primary of the ideal transformer is interrupted by the secondary switch.

With the switch moved, the PWM model now appears in its proper form, enclosed by the gold outline. We can now replace the switches with the linearized AC model shown in blue, and circuit analysis can continue. The only difference in this circuit from the buck equivalent model is that there is now a transformer applied across the input voltage. Apart from that, the subcircuit for the PWM switch is unchanged from those of **Figure 3**.

Figure 5 shows how the flyback converter is rearranged to reveal the PWM switch. First, we add the primary side inductor explicitly to the circuit. This component can then be reflected through to the secondary as shown, with its value reduced by the square of the transformer turns ratio.

Then we can push the switch itself through the transformer. Once we have done this, the PWM switch appears and can then be replaced with the AC

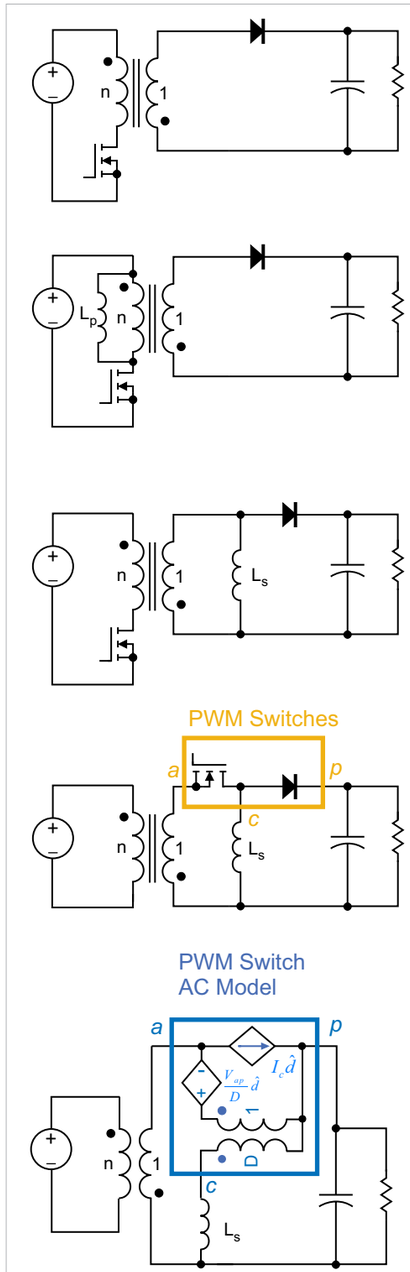

Figure 5: Rearrangement of the flyback converter puts the inductor on the secondary side.

small-signal circuit model.

I have yet to encounter a PWM converter that cannot be quickly rearranged to reveal the PWM switch, and hence be easily amenable to analysis with the PWM switch model. In [2], it was shown how this could be done for the Sepic converter. In the next part of this article, we will tackle some more challenging circuits with tapped inductors.

Summary

There are many new faces coming into the world of power electronics and power supply design. They often have new and useful skills to bring to our field, but have not had time to study the fundamentals of power supply analysis. This is a natural evolution in any field, and new engineers need to search on their own for solutions.

The PWM switch model was discussed in great detail when it was first discovered at conferences and in industry papers, but is now assumed to be background knowledge. I often find that many of our workshop attendees [3] are not aware of the existence of these modeling tools, and it is important to introduce them to the simplicity of PWM switch model application to their circuits.

References

1. Boost and Buck-Boost Converters with Voltage-Mode Control, Articles [17,19], http://www.ridleyengineering.com/design-center.html
2. Analyzing the Sepic Converter, Article [02], http://www.ridleyengineering.com/design-center.html
3. Power Supply Laboratory Workshop, http://www.ridleyengineering.com/workshops.html
4. To learn how to make control measurements, please visit http://www.ridleyengineering.com/analyzer.html
5. Join our LinkedIn group titled “Power Supply Design Center”. Noncommercial site with over 2200 helpful members with lots of experience.

www.ridleyengineering.com

Addressing 400-Vdc power in advanced industrial and data-center apps

Simplified power supply chains demand increased performance from board-level power

By: Steve Oliver, Vicor

In any operating system, distribution losses are a significant factor in overall system efficiency at every level. In the case of telecom central office applications, traditional 48Vdc systems become very expensive to install (due to increased copper cost and weight) and run (due to I2R loss) while in large data centers, traditional AC distribution with the related Uninterrupted Power Supply (UPS) equipment infrastructure requires superfluous conversion stages, leading to low system efficiency using more complex equipment, with subsequently less performance (in MFLOPS) per each and every expensively air-conditioned square foot of real estate.

Within the walls of a datacenter, the 19th-century debate between Tesla and Edison over AC vs. DC power distribution at the grid level, covering technical, political, and commercial concerns, has been re-opened by the 21st century catalysts of global warming, the cost of electricity, and renewable energy sources. The blurring and/or merging of the traditional server & telecom sectors into what is now commonly referred to as 'datacom', the demands of the 'Exascale Challenge', and consumer-driven 'triple-play' (voice, video, internet) services have accelerated the move to higher-efficiency systems. This has raised the argument over power distribution again, as full-scale 400VDC-based datacom installations have yielded between 8% and 10% energy savings[1].

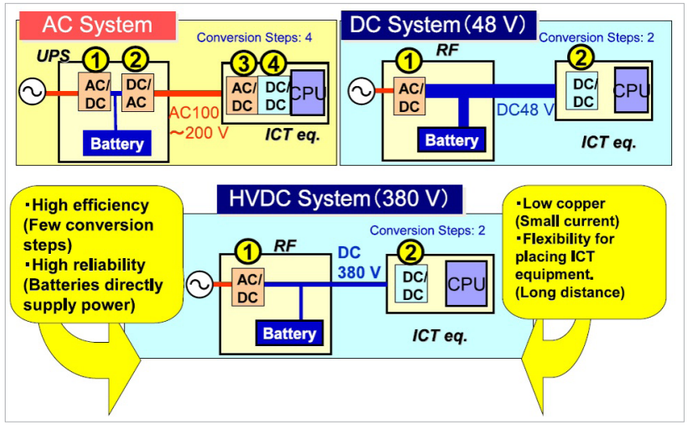

Figure 1: A high-level architecture simplification of 400VDC distribution

A 400Vdc system (also referred to at 380Vdc) offers several advantages to the data center. The largest advantage is the streamlining and simplification of the power system, reducing the components, the related parasitics & leakages involved in them, and the connection & mounting infrastructure. In addition, fewer conversion steps also mean a higher level of system reliability as well as a lower materials cost (in very expensive and heavy devices). No synchronization is needed to use (often incentivized) wind, solar and/or other grid-interactive power at the right time (with less dependency). Plus, no phase balancing / harmonic problems exist and there is no stranded power due to equipment de-rating.

Benefits within and beyond the data center

DC-based power architectures benefit more than data centers. Power distribution within office buildings and retail stores is also undergoing a transition, with 380VDC infrastructures offering a 5% direct efficiency saving, plus additional savings from easier integration of intelligent building sensors, controls, network protection and network-stabilizing interfaces[2]. **Figure 1** outlines the high-level architecture simplification using 400Vdc distribution[3].

Considering that only a ridiculously small amount of the power in a data center actually gets to the systems actually involved with performing the work, any added efficiencies in the infrastructure systems pays off exponentially in ROI and system reliability. At the package and board level, the advantages continue, with less copper required for lines able to run longer distances and the elimination of duplicated power stages. Increased efficiency also means less waste heat, with the related advantages of lessened thermal impact on components and reduced cooling requirements at every level.

While 400Vdc-based power distribution trials indicated promising commercial value over the last decade, including Intel's LBNL trial in 2007 plus dedicated pioneering work from NTT, there were many hurdles to adoption, including a lack of standards, metrics, distribution hardware (connectors, power strips, etc.) and power converters. These barriers hindered engineers from testing and deploying 400Vdc-based systems in the past.

The tipping point has occurred within the last two years, starting with ITU and ETSI published standards and working groups including IEEE, NFPA, Emerge Alliance, etc.[4] and concurrent installation work at NTT, Hitachi, Orange and China Telecom. Note that while in general discussion, "400Vdc" and "380Vdc" have been used interchangeably, when referring to the voltages in detail, 380V is the nominal (normal operation) reference voltage and 400V is a maximum operating voltage condition.

Intelec 2012 saw a collaborative 400Vdc power distribution and conversion hardware demonstration[5]. This employed AC to 400Vdc and 400V to 12V, 48V converters plus associated connectors, power strips and even 400VDC LED lighting fixtures from established industry names such as Emerson, Vicor, Fujitsu, Anderson, GVA and Philips. While 400VDC distribution technology is established, the vast majority of data center loads (switches, routers, servers, storage) requires the legacy 12V or 48Vdc input. As a result, the power conversion stage requires further examination, including a focus on the input voltage variability and output voltage regulation requirements.

To address this new market opportunity, Vicor has created the ChiP (Converter housed in Package) family of board-level 400Vdc-input power converters, based on proven conversion technology introduced in 2003. ChiP converters are suitable on their own for 12-to-48Vdc legacy loads as well as serving in a power solution for next-generation systems drawing as low as one volt.

ChiP technology[6] is a major step in power conversion efficiency (%) and density (W/in^3) with a manufacturing flow akin to semiconductor 'chip-scale' packaging techniques. With CHiP, all of the manufacturing PCB panel is utilized and the individual components are sawn into 'ChiP-scale' power devices. Combined with advanced design techniques and latest generation active silicon components, ChiP converters enable unprecedented performance without resorting to nascent, unproven semiconductor materials.

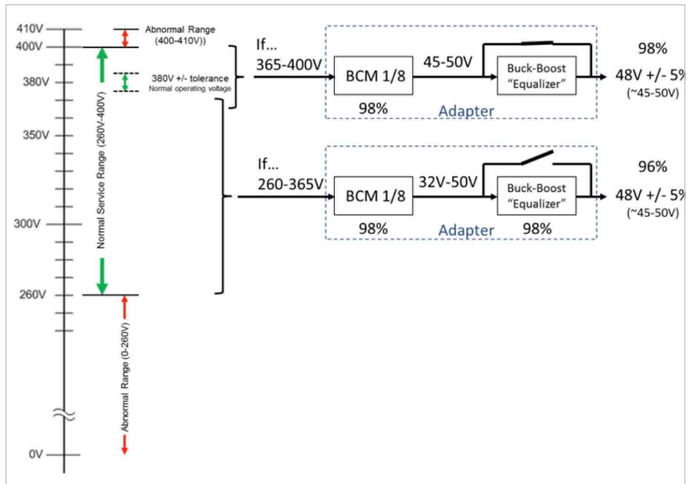

Figure 2: ETSI 'Adapter' maintains maximum conversion efficiency over the whole input range.

The first ChiP example uses the Sine Amplitude Converter (SAC) ZVS, ZCS DC-DC bus converter to convert from nominal 384VDC direct to 12V or 48V using a fixed ratio, isolated, fixed-frequency, LC-resonant transformer.[7,8] The 6123 (61 x 23mmm as sawn) package is capable of 1,500W at up to 98% efficiency, with a resulting power density of over 2,000W/in^3.

To continue the power conversion story, we must first consider the input and output voltage requirements. In systems with a tightly regulated 380V input, a fixed-ratio converter creating a simple 12V (or 48V) rail gives the highest efficiency, smallest size result. However, if the input voltage varies (e.g. if the AC line fails and energy storage at 400V starts to decay (down to as low as 260VDC in the ETSI case), a regulating stage is required to maintain the output voltage and enable a controlled shut-down of the system to maintain task- or data-integrity. In this case, a housekeeping system monitors the ~380V rail and inserts a regulating stage, as shown in **Figure 2**.

Here, the regulating 'equalizer' is 3623 ChiP non-isolated, ZVS buck-boost converter, with up to 98% efficiency and >2,500W/in^3 power density. With this small, yet efficient combination of converting devices, the question of power conversion location is opened up. Now, the 400V-12V/48V converter can be placed in a 'drop-box' on the bus bar, within a power strip, or even on the motherboard of the server/switch/router load. This completely eliminates traditional silver-box power supplies and frees valuable rack real estate for additional switching/routing/processing hardware, increasing the MFLOPS/sqft metric.

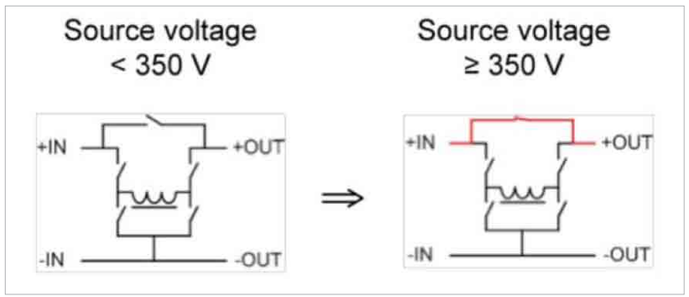

Figure 3: Vicor equalizer concept addresses different system voltages

Maintaining a stable output

In any power distribution infrastructure, maintaining a stable output under varying input conditions is paramount. The proper circuit cannot add too much cost and complexity to the solution or it becomes unfeasible. In this case, a microcontroller-supervised housekeeping circuit in the power chain monitors the input voltage and kicks in a regulator in circumstances where the voltage drops below 380V. With Vicor's Equalizer in the powered equipment power supply chain, there is no efficiency penalty in supporting the ETSI EN 300 132-3-1 normal service voltage range of 260V - 400V DC.

The "Equalizer" block enables the use of a high-voltage bus converter as equipment front-end element, with minimal impact on conversion efficiency. During normal operation with a source voltage greater than 350Vdc, the equalizer is bypassed and does not impose any losses in the power transfer. The equalizer is activated only when the source voltage drops below the 350V DC level (typically during battery discharge). Efficiencies in such systems are usually as high as 98% under normal operation, and in the circumstances where the housekeeping circuitry is employed, efficiencies can remain as high as 96% (see **Figure 3**).

With the agreement on 400Vdc standards and the availability of power distribution and conversion hardware, major savings can be enabled across the industry. In 2010, data centers alone used about 1.3% of the world's total electrical energy (or 250B kWhr/yr)[9]. The efficiency advantages of 400Vdc systems have the potential to save $9B/yr (€5B) across the industry. Savings from industrial, commercial, retail real installations would add to that financial figure. Concurrently, 16M tons of CO_2 could be eliminated and 15M barrels of oil saved per year[10].

The current state of 400Vdc-based is no longer a curiosity or intellectual exercise, but a reality that must be addressed by the design community. Solutions such as the ChiP bus converters and buck-boost regulators can significantly simplify the creation of power systems serving the next-generation industrial and datacom marketplace.

References

1. France Telecom (Orange), China Mobile
2. DCC+G (DC Components and Grid) consortium including Emerson, Siemens, Philips, Infineon Technologies, based at the Fraunhofer Institute (Erlangen, Germany) and funded by ENIAC (European Nanoelectronics Initiative Advisory Council) and the German Federal Research Ministry
3. Image reference: "Grounding concept considerations and recommendations for 400VDC distribution system" Hirose, Tanaka, Babasaki (NTT), Person, Foucault (France Telecom), Sonnenberg, Szpek (Emerson Network Power), Intelec 2011
4. International Telecommunication Union (ITU-T) standard L.1200 (May 2012), European Telecommunications Standards Institute (ETSI) EN 300 132-3-1 (February 2012), IEC (SG 4): LVDC DISTRIBUTION SYSTEMS UP TO 1500V (October 29th 2012, Berlin, Germany) - information exchange with IEC-ITU-ETSI-IEEE-Emerge Alliance. Working groups / collaboration between IEEE, Emerge Alliance, NEMA / EPRI, NFPA, ATIS, etc.
5. M.Salato, A.Zolj, of Vicor, D.Becker and B.J.Sonnenberg of Emerson Network Power, Energy Systems "Power System Architectures for 380VDC Distribution in Telecom Datacenters", Intelec 2012,
6. ChiP technology background: http://www.vicorpower.com/promotions/AC_to_PoL/ChiP_Technology/lp.php
7. Sine Amplitude Converter (SAC) topology video: http://player.vimeo.com/video/24284299
8. Sine Amplitude Converter (SAC) white paper: http://www.vicorpower.com/cms/home/technical_resources/white-papers
9. Jonathan Koomey. 2011. Growth in Data center electricity use 2005 to 2010. Oakland, CA. http://www.analyticspress.com/datacenters.html
10. S.Oliver, Vicor: "Kyoto, Copenhagen and the European 20-20-20 Energy Strategy: Using 400VDC Distribution to Save Energy and Make Money", Electronica 2010. http://www.vicorpower.com/promotions/2012/AC_to_PoL/Webinar/Rebroadcast/20-20-20_Energy_Strategy/dc.php

www.vicorpower.com

Transient thermal resistance (Zth) of power modules determined by simulation and measurement.

The Zth of a power module is used to calculate device lifetime

By: Dr. Krzysztof Mainka, Dr. Markus Thoben, Infineon Technologies

The transient thermal resistance (Zth) of a power module describes a key performance that is used to estimate the maximum output current for transient loads. It can also be used to calculate the temperature ripple as with a mission profile and resultant the lifetime of the power module. When dimensioning a power electronics system, the transient thermal resistance (Zth) of a power module is required to calculate the lifetime. The Zth has a significant influence if different power modules are investigated in the same application, as the heat capacity reduces the temperature ripple for a limited time. Precision and accuracy is required to calculate the correct temperature ripple.

Simulation and VCE(T)-measurement based Zth are used to calculate the temperature in an IGBT module after short pulses with high peak losses. The temperature gradient shows significant differences, and only simulation-based Zth agrees well with the test results from

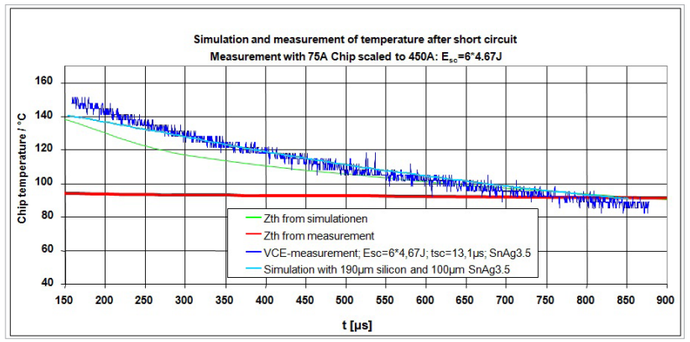

Figure 1: Comparison of measurement with FEM-Simulation and calculation results

short pulses. Delays between switch-off of load current and the start of measurements in large power modules have a significant impact on the short-time thermal resistance. Depending of inverter output frequency, the deviation in short-time thermal resistance influences the calculated temperature ripple, and therefore the predicted lifetime. Making use of Finite Elements simulation to determine the transient thermal resistance Zth ensures the correct calculation of short-time thermal behavior for the lifetime prediction.

Determination of transient thermal resistance Zth

According to e.g. JEDEC standard (JESD24-12), in the measurement of an IGBT, the temperature-dependent forward voltage drop for a small sense current is measured after heating the device with a load current. To measure the transient temperature behaviour, the cool-down phase is checked to determine a virtual junction temperature, which represents the average temperature distribution in the chip. As a second method, FEM-Simulation can be used to calculate the Zth. 3D CAD-Data and material properties are used to simulate the transient temperature distribution and extract the average temperature in the chip.

Differences between measured and simulated Zth

A simulation of the short puls test with Zth Foster models derived with simulation and measurement methods is performed. The calculation results are compared with extrapolated measurement results of the temperature after a short pulse with high peak losses with a single chip. Only the Zth Foster model derived from simulation shows good agreement with the measurement. Better results can be only achieved with direct FEM-Simulation as shown in **Figure 1**.

Simulating the Zth measurement process gives an explanation for the deviations. As shown in **Figure 2**, during the measurement process a linear extrapolation for the short time is per-formed.

The simulation result shows a strong change of temperature gradient (up to 1ms), resulting from varying thermal properties in the stack consisting of silicon solder and copper in the top part of the stack. The resulting negative offset reduces the Zth,jc in the short-time. To check whether further factors cause deviations between simulation and measurement based Zth,jc curves, the influence of the offset is investigated. In **Figure 3** the Zth,jc derived from measurement data is corrected with the offset calculated in **Figure 2**.

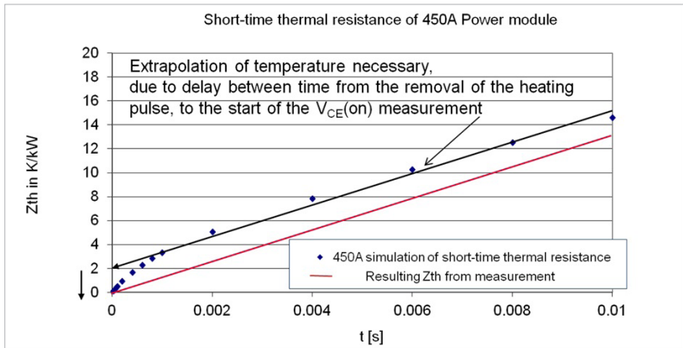

Figure 2: Comparison of simulation and experiment at short-time thermal resistance: extrapolation to compensate delay in measurement results in negative offset

Correcting the offset this results in good alignment with Zth,jc from simulation. Consequently no further effects are creating deviations between measurement and simulation of the transient thermal behavior.

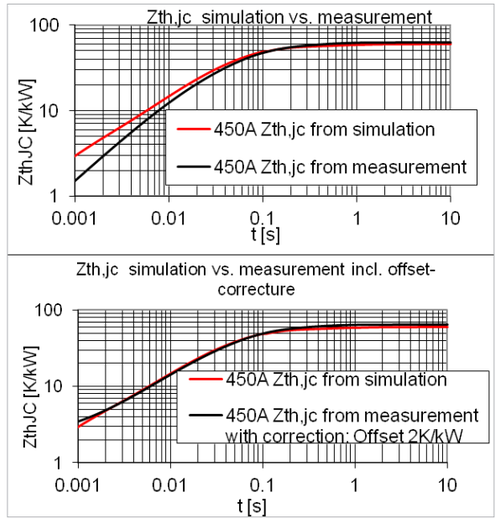

Figure 3: Comparison of Zth,jc from simulation vs. experiment without and with offset correction

Influence on the temperature ripple and life time

The influence of deviation between Zth from simulation and measurement on the temperature ripple during inverter operation is investigated in two cases. In the first case a typical three phase inverter configuration under the assumption of sinusoidal output currents at inductive loads is considered. The junction temperature therefore oscillates with the output frequency.

Although for selected operation conditions the average losses might be the same, the ripple and therefore the peak junction temperature increases at lower frequency and decreases with higher frequency.
Based on the power cycling curves for IGBT4, a pos-

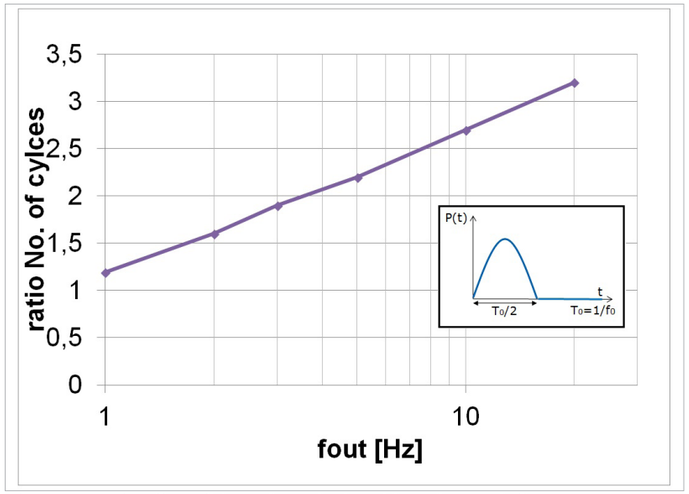

Figure 4: Ratio of possible cycles calculated based on Zth from measurement to possible cycles calculated based on Zth from simulation

sible number of cycles for the different temperature ripples was calculated, where ΔT less than 10K for frequencies greater than 20Hz were neglected. Calculation results as a ratio of possible cycles calculated based on Zth from simulation to possible cycles calculated based on Zth from measurement are shown in **Figure 4**. The lifetime calculation based on Zth from measurements for frequencies greater than 1Hz seems to be more optimistic. This corresponds, however, to the part of the Zth, which in measurements is inaccurate.

Because for frequencies greater than 20Hz the temperature ripple is negligibly small, in the second case, a rectangle load current shape to represent the varying load profile was used. When changing the duration of the pulse (ton) resulting temperature ripples and possible numbers of power cycles were calculated based on Zth from simulation and measurement. A ratio of possible number of cycles is shown in **Figure 5**. In both cases, the lifetime calculation based on Zth from measurements for ton times of less than 1 second (or frequencies greater than 1Hz) looks more optimistic. Determining lifetime on the basis of Zth from extrapolated measurements will predict too optimistic results if the mission profile contains a lot of short power pulses with significant amplitude. However, for many common applications relevant load pulses are generally longer than 1 second, which does not affect the calculation error of lifetime.

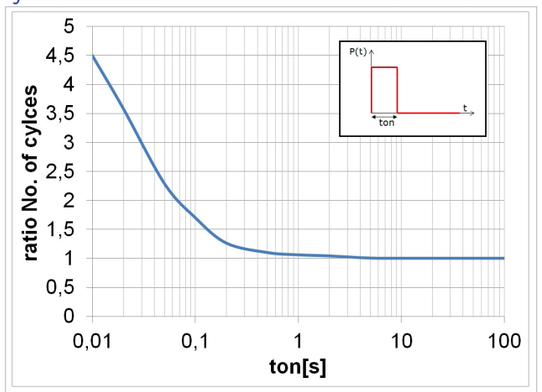

Figure 5: Ratio of possible power cycles calculated based on Zth from measurement to Zth from simulation

A precise transient thermal resistance (Zth) is required to calculate the temperature ripple as a result of a mission profile, especially for low inverter output frequency. The delay time between removing the heating and starting the VCE measurement and additional noises on the measurement signal requires an extrapolation. This results in a negative offset, when measuring the Zth with the VCE method and applying a linear extrapolation. Making use of Finite Element simulation to determine the transient thermal resistance Zth ensures a correct calculation of short-time thermal behavior for the lifetime prediction.

www.infineon.com

USB power sensors in RF power measurement

It's easy to set up communicate with USB-interface test instruments

By: Chin Aik Lee, Agilent Technologies

In many of today's RF power measurement applications there is a need to make multiple power measurements simultaneously. Added complexities occur when the measurements need to be obtained from places where access is inconvenient, or when the distance to the measurement location exceeds the IEEE industry-specified USB cable length of 5 meters (16 feet).

For instance, a base station commonly includes a compact equipment shelter or outdoor enclosure panels along with antennas that may be mounted on a roof, the wall of a building, or on a free-standing mast. A given base station may operate on several channels (typically two or three), where each channel uses a specific set of frequencies: one for the uplink and one for the downlink. Depending on the communication technique, each channel can simultaneously process communications from one or several active handsets.

These sites require routine maintenance and present several challenges. The distance between the antenna and control room may necessitate that measurements be obtained over distances beyond 5 meters and sometimes as far as 50 meters. Measurements may be required from different power sensors and at hourly, daily or monthly intervals.

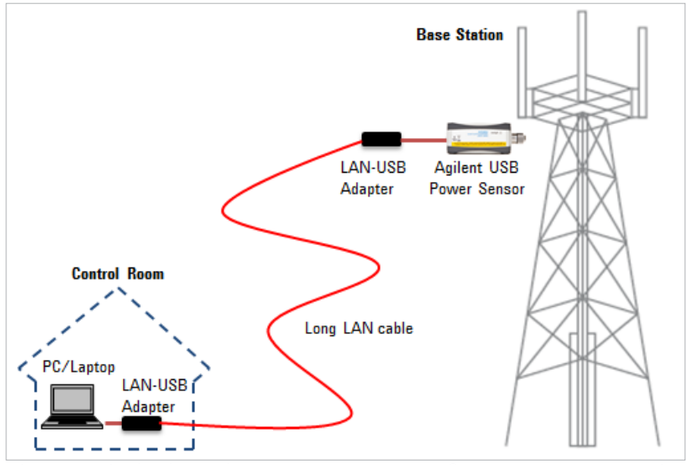

Figure 1: Single-channel power measurement of USB power sensor using LAN-USB extender to extend the measurement distance for base station antenna application

Traditional RF power-measurement methodologies require you to connect a power sensor to a power meter. As a result, the setup for multi-channel power measurement demands plenty of rack space to accommodate both the power meter and the power sensors. This situation increases the costs of a test system significantly.

USB power sensor solution

To address such challenges, using USB power sensors is an ideal power measurement solution for measuring the transmitter/receiver power of outdoor base stations for system characterization. Its small form factor is convenient for site technicians who need to climb the antenna for installation and maintenance. In situations where the USB cable length must exceed 5 meters, USB extenders allow the

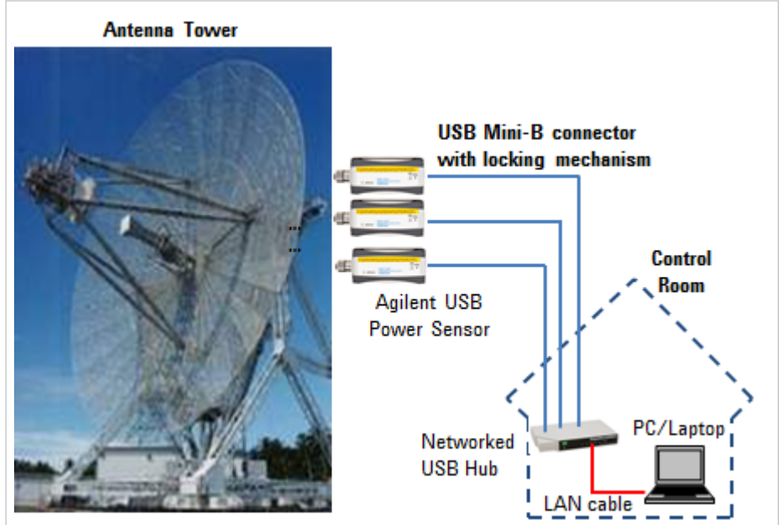

Figure 2: Multi-channel measurements via networked USB hub for simultaneous antenna measurement

USB protocol to be transmitted via a LAN cable for single-channel power measurement (see **Figure 1**).

A USB extender consists of a transmitter and a receiver that are interconnected by the LAN cable. This allows data to be transferred at distances up to 100 meters These USB extenders are plug-and-play and work efficiently with all major operating systems. For long-distance applications where multiple power (multi-channel) measurements must be made simultaneously, multiple USB power sensors can be connected to a USB hub installed at the base station and networked to the control room (see **Figure 2**).

Figure 3: USB power sensors

The USB power sensor is a combination of a power meter and a power sensor that converts RF and microwave power directly into digital data, and allows this data to be analyzed using a software application, such as Agilent's Power Analysis Manager. The power-measurement readings are retrieved using standard SCPI commands or VIV-COM/IVI-C drivers. The SCPI-based command set provides a user-friendly programming environment and allows the use of the same method of communication for both the power sensor and the power meter. (See **Figure 3**.)

Using a networked 5-Port USB hub

Using a LAN to communicate with USB-interface test instruments allows an engineer to control and program the instruments remotely without connection-distance limitation. A networked 5-port USB hub allows multi-channel power measurements to be taken simultaneously when multiple USB power sensors are connected to the networked hub.

The networked 5-Port USB hub uses USB over an IP connection (LAN) to overcome the distance limitation. The USB power sensor can be remotely controlled from a PC or laptop via LAN. The networked 5-port USB hub can connect up to five units of the USB power sensors. (See **Figure 4**.)

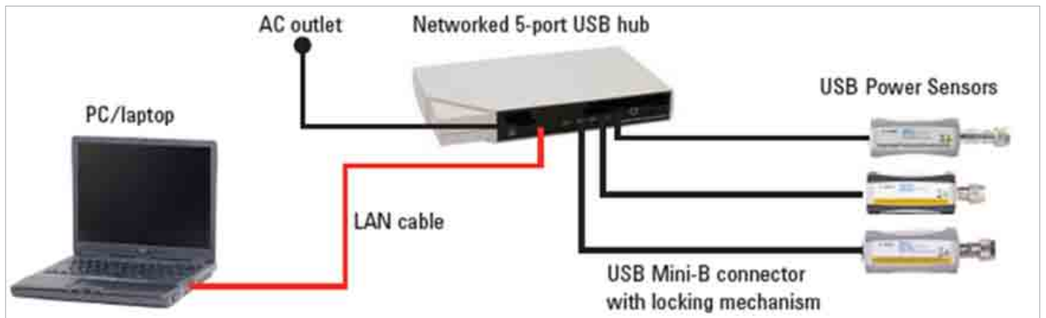

Figure 4: USB power sensors and networked 5-port hub setup diagram

Extended Distance Single-Channel Power Measurement with USB Extender

Users of USB peripheral devices are often challenged to overcome the 5-meter limitation of standard USB cable, as some applications require longer connections. A USB extender boosts the distance of a USB peripheral device by up to 100 meters from a host computer using a regular LAN cable. A USB extender has a built-in buffer and actively regenerates signals to preserve data integrity. It consists of a transmitter and a receiver module (see **Figure 5**). The USB extender is self-powered and so it does not require an AC adapter. It is a truly plug-and-play passive device without required driver installation and supports USB 1.0, 1.1, and 2.0 standards with data transfer rates up to 480 Mbps (depending on USB extender specification).

Figure 5: USB extender with built-in USB cables, a transmitter, and a receiver module

For long-distance applications where the power measurement (single or multiple) must be made from the place access is inconvenient such as outdoor base station antenna, USB power sensors would be an ideal solution without the need for a separate power meter. To overcome the 5-meter length issue, a USB extender or USB networked hub can be remotely located up to 100 meters (depending on the USB extender and networked hub) from the host computer. (See **Figure 6**.) This allows the user to extend USB power sensor over LAN cable and remotely acquire the power measurement via a designated Windows application. This is a cost-effective solution and easy to implement.

www.agilent.com

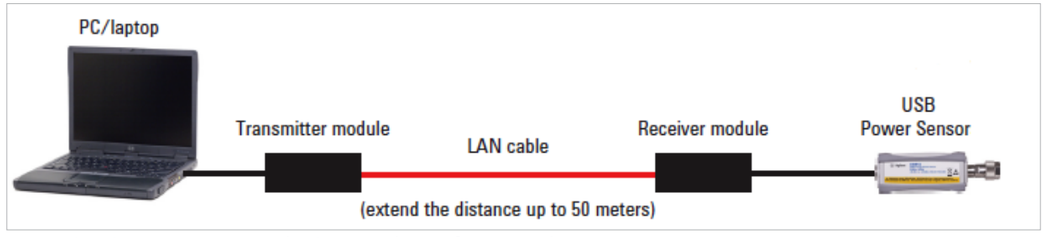

Figure 6: USB power sensor and USB extender configuration diagram

Using an isolated error amplifier to replace an optocoupler and shunt regulator

A loop bandwidth of over 250 kHz can be achieved

By: Brian Kennedy, Analog Devices

Designers of isolated AC/DC, DC/DC or DOSA compliant power modules face challenges when responding to market requirements for increased performance. This article introduces the digital isolator error amplifier which improves transient response and operating temperature range for primary side control architectures. The traditional application for a primary side controller is to use an optocoupler to provide feedback loop isolation and a shunt regulator as an error amplifier and reference. While often seen as an inexpensive isolator for use in a power supply, an optocoupler will limit the loop bandwidth to a maximum of 50 kHz, and in practice it can be much lower. The use of fast and reliable digital isolator circuits, which integrate an isolated error amplifier and precision reference functions into a single package, will result in a precise isolated error amplifier with much lower temperature drift and much higher bandwidth. A loop bandwidth of over 250 kHz can be achieved by an isolated error amplifier, which

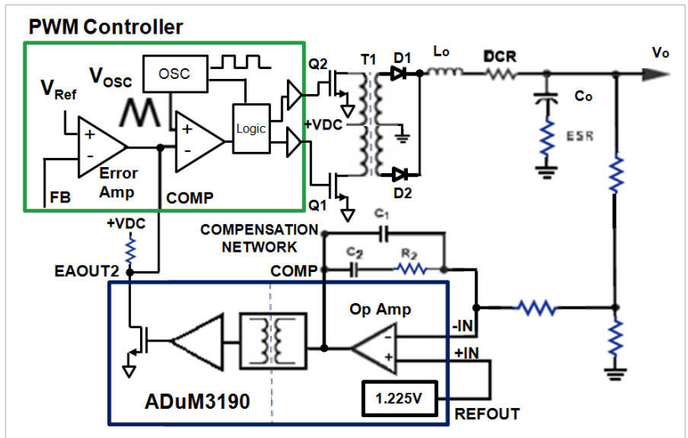

Figure 1: Block Diagram of a Flyback Regulator with Optocoupler and Shunt Regulator

makes it possible for isolated primary power supply designs to run at much faster switching speeds. With the right power supply topology, faster switching speeds enable the use of a smaller output filter inductor and capacitor for a more compact power supply.

The initial topology we will examine is a flyback converter, since this is the simplest circuit in terms of components count. The flyback circuit can have the fewest switches, in this case just one on the primary side, and a rectifying diode on the secondary side. The simple flyback circuit is often used for relatively low output power, but it does have a high output ripple current, and low crossover frequency due to the right half-plane (RHP) zero. As a result, flyback circuits require large values of output capacitance with a large output ripple current rating. The optocoupler approach is shown in **Figure 1** and involves the use of a shunt regulator to act as the error amplifier of the feedback voltage

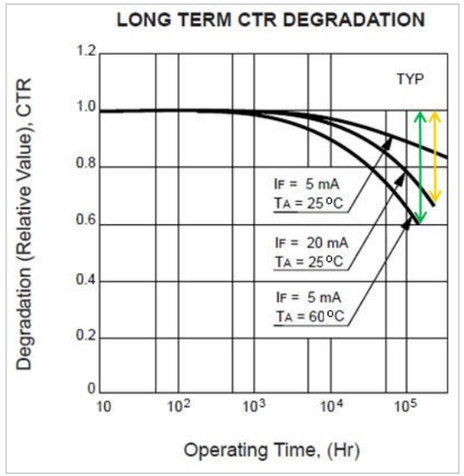

Figure 2. Optocoupler CTR Degradation

of an isolated output voltage VO. The shunt regulator provides the reference voltage with a typical 2% accuracy when used as the accuracy standard. The divided down output voltage is compared to the shunt regulator's reference voltage by the internal error amplifier and the output is fed to the optocoupler LED circuit. The optocoupler LED is biased by a current provided by the output voltage and a series resistor and the amount of current needed is based on the optocoupler current transfer (CTR) characteristics as described in its datasheet.

The CTR is the ratio of output transistor current to input LED current. The CTR characteristics are not linear, and vary from optocoupler to optocoupler. As shown in **Figure 2**, optocoupler CTR will vary over operating lifetime, which makes designing for reliability very challenging. The optocoupler you design and test today will usually have a two to one uncertainty in initial CTR, and will have 40% less CTR after years of use or service in high temperature environments found in high power and high density supplies. When an optocoupler is used as a linear device, it has a relatively slow transfer characteristic (the small signal bandwidth is about 50 kHz) which leads to slow loop response of the power supply. For the flyback topology, having slow transfer characteristics may not be a problem, since this topology requires that the compensation of the error amplifier reduce the loop bandwidth to maintain a stable output. The concern with the optocoupler is that the variation of its output characteristics over time can force the designer to reduce the loop response even more to ensure the stability of the loop. The disadvantage of slower loop response is that this will degrade the transient response, and the output voltage

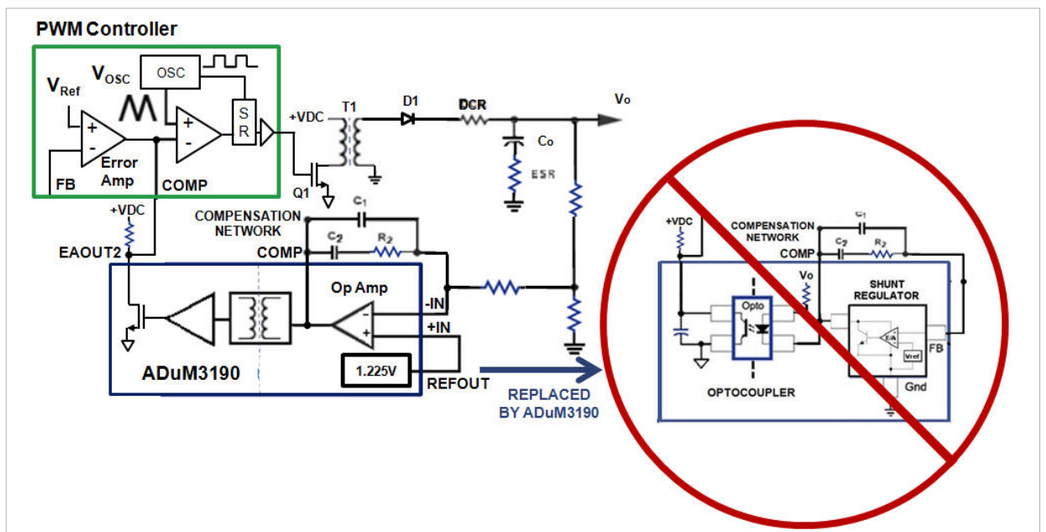

Figure 3. Isolated Error Amplifier replaces Optocoupler and Shunt Regulator

will take a longer time to recover after a load transient. Adding a larger output capacitance can help reduce the output voltage drop, but will increase the output response time. This leads to a larger and more costly power supply design, when a smaller and lower cost solution may be possible and more desirable.

Having illustrated the difficulties of obtaining stable operation of an optocoupler as a linear isolator, the ability of the isolated error amplifier to offer stable and reliable performance over time and temperature extremes can be examined. As shown in **Figure 3**, the shunt regulator and VREF function are now replaced with the wideband operational amplifier and 1.225 V reference section and the optocoupler is now replaced with the fast linear isolator based on digital isolator technology. The operational amplifier on the right side of the device has a noninverting +IN pin connected to the internal 1.225 V reference and an inverting –IN pin available for connecting a feedback voltage in an isolated dc-to-dc converter output, through a voltage divider. The COMP pin is the operational amplifier output, which can be used to attach resistor and capacitor components in a compensation network. The COMP pin internally drives the transmitter block, which converts the operational amplifier output voltage into a modulated pulse output that is used to drive the digital isolator transformer. On the left

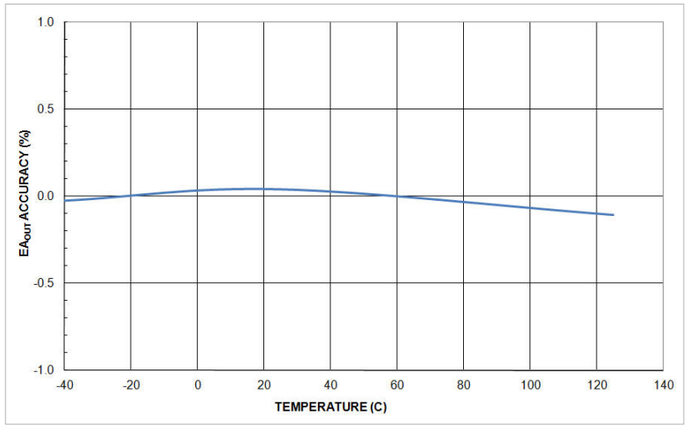

Figure 4. Isolated Error Amplifier Output Accuracy Vs Temperature

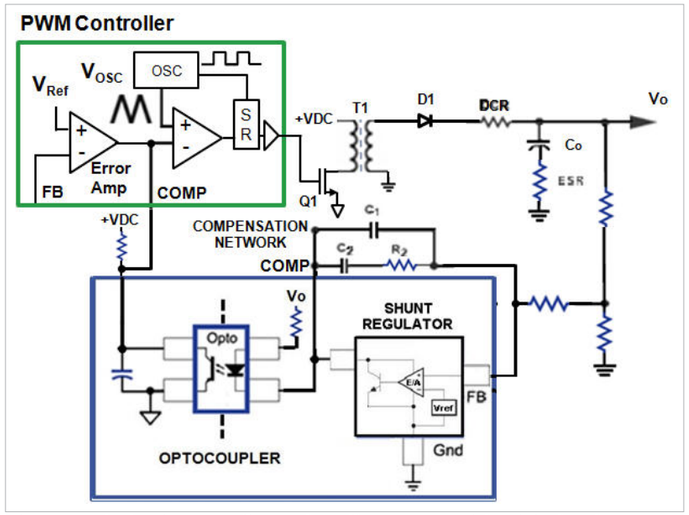

Figure 5. Block Diagram of a Push Pull Converter with Digital Isolator Error Amplifier

side of the isolated error amplifier, the transformer output signal is decoded and converted into a voltage that drives an amplifier block. The amplifier block produces the error amplifier output available at the EAOUT pin, which is used to drive the input of a PWM controller in the dc-to-dc circuit.

The advantages of this new isolated error amplifier include the reference and operational amplifier, which have been designed to minimize offset and gain error drift over temperature. The 1.225 V reference circuit is trimmed for 1% stability over temperature, which is more accurate and has much less drift than a shunt regulator. As shown in **Figure 4**, the typical output characteristic of the isolated

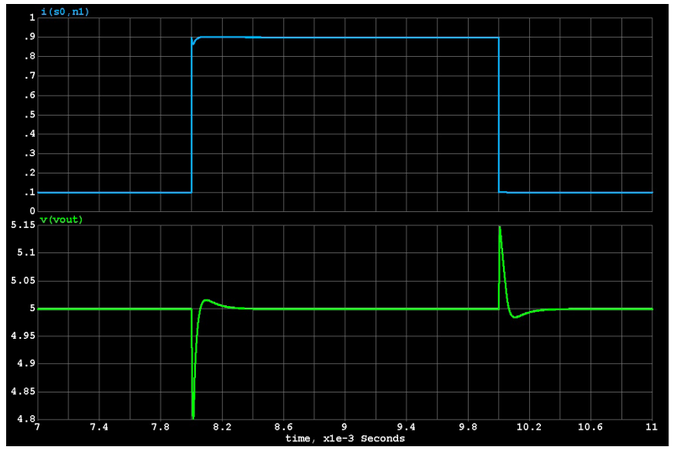

Figure 6. Push Pull Converter with Digital Isolator Error Amplifier 100mA to 900mA Load Step

error amplifier changes only 0.2% over a -40 to 125°C range, enabling a high accuracy DC/DC output. To maintain a stable output characteristic, the COMP output of the operational amplifier is pulse encoded to send digital pulses across the isolation barrier and then decoded back by the digital isolator trans-former block to an analog signal, completely eliminating the problems from CTR variations when using an optocoupler isolation.

For applications requiring faster transient response than possible with a flyback circuit, a push-pull topology can be implemented with the isolated error amplifier. The push-pull circuit is shown in **Figure 5**, with two MOSFETs alternately switching on and off, charging the two primary windings of a transformer, and then the two secondary windings with diodes to conduct and charge the output filter inductor and capacitor. When properly compensated, the push-pull topology will be very stable with much faster switching frequencies and faster loop response. The same isolated dc to dc design example used for the flyback circuit, 5 V in to 5 V out at 1.0A output current, is now implemented for the push-pull circuit using the ADuM3190 isolated error amplifier. The push-pull design has a 1.0 MHz switching frequency versus the slower 200 kHz of a typical flyback design, so the ADuM3190, with its higher bandwidth, presents a better option than an optocoupler. The output filter capacitance has been reduced from 200µF for a typical flyback down to only 27µF for the push-pull, and a small 47µH inductor is added. The waveforms shown in **Figure 6** show that for the conditions of 100mA to 900mA load step, the push-pull circuit with the isolated error amplifier responds in only 100 µsec as compared to 400 µsec for a typical flyback, a four times improvement. Instead of a 400 mV change in output voltage seen by the flyback circuit, the push-pull circuit output voltage only changes by 200mV, a two -old improvement. The use of the faster push-pull topology and the higher bandwidth of the isolated error amplifier, results in high performance with faster transient response and a smaller output filter.

These improvements were made possible by the high bandwidth of the 400 kHz isolated error amplifier, which enables a faster loop response. The secondary side error amplifier, which has a high gain bandwidth product of 10 MHz, is about five times faster than a shunt regulator, and enables the higher switching frequency to 1.0 MHz for an isolated dc to dc converter. Unlike optocoupler solutions, which have an uncertain current transfer ratio over lifetime and over temperature, the isolated error amplifier has a transfer function that does not change over its lifetime and is stable over a wide temperature range of –40°C to +125°C. With these performance improvements, the isolated error amplifier will become the solution of choice for power supply designers of isolated DC/DC converters, who want to improve transient response and operating temperature range with primary side control architectures.

www.analog.com

LED operating capacity is a major factor in system ROI

LED efficacy is improving as powerfully as the previous evolution of the microprocessor

By: David Cox, Don Hirsh, Michael McClintic, Cree

In the evolution of electronics there have always been faster, more powerful, or more compact processors. LED efficacy has been improving as powerfully as the previous evolution of the microprocessor, but LED-based illumination designs are not consistently taking advantage of new capabilities. Advances in the production of lighting class, high power LEDs should cause the lighting industry to reassess how to create cost-optimal LED-based designs. Several advanced LED manufacturers, including Cree, Inc., have developed a large and expanding body of information concerning performance maintenance of LEDs over time and temperature.

This knowledge of long-term behavior is now standardized in LM-80 data sets (lumen maintenance and color shift) and TM-21 projections. For Cree, this information shows, in the highest quality parts and in well-designed systems, LEDs can operate at high current and high temperature levels with fewer performance penalties than ever before. This same data calls into question the initial design and driver methodology that builds

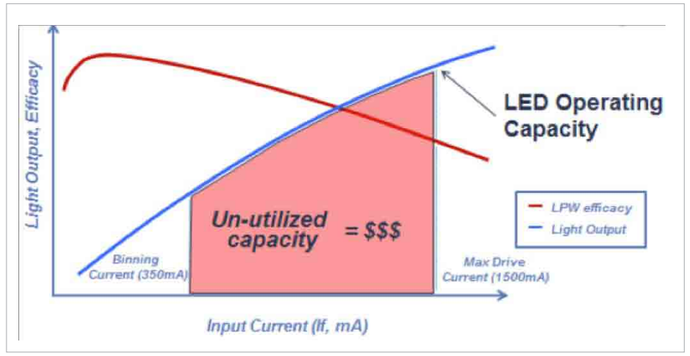

Figure 1: Flux and Efficacy Over Current Show Substantial Available Operating Capacity

systems in and around binning currents rather than over a wide range of drive currents and temperatures. Using LEDs at higher operating capacity can deliver more lumens per-LED with a correspondingly reduced system cost. For many lighting applications, more aggressively priced products can be created with a reduced component count and associated higher operating temperatures and lower efficacy. Taking full advantage of an LED's operating capacity becomes an attractive option for applications requiring maximum lumen output at a reduced cost.

Previously, a conservative design strategy was appropriate for a relatively young technology (like packaged high power LED components). We now know more aggressive designs are desirable and appropriate for cost-efficient performance. For lighting class LEDs, that is. In LEDs that maintain chromatic and luminous stability, there is an abundance of unused lumens available to thoughtful systems designers. With the operating temperature held constant, we can visualize this unused capacity in **Figure 1**. When driven at binning current, the LED is using less than 25% of its rated capacity. The other 75% is bought and paid for, but under-utilized.

LED system designs have often been created with drive currents in and around LED binning currents. This is both an industry-wide habit and an engineering-conservative approach to system reliability. But the new data shows that much more aggressive drive currents and temperatures are possible without sacrificing long-term reliability. Reduced system costs are the benefit of this new approach.

Current	Ta/Tsp	Test Duration	α	β	Calculated $L70^2$	Reported $L70^2$
1000 mA	85°C	8,568 hrs	9.531E-07	9.891E-01	363,000 hrs	L70 (9k) > 51,400 hrs
1000 mA	105°C	8,568 hrs	3.300E-06	9.886E-01	105,000 hrs	L70 (9k) > 51,400 hrs
1500 mA	85°C	8,568 hrs	2.174E-06	9.971E-01	163,000 hrs	L70 (9k) > 51,400 hrs

Table 1: TM-21 Projection for Cree XLamp® XP-G LED

LM-80 data sets used to create TM-21 projections are the reliable and standardized method that allows predictions for any given LED in a systems context[1]. As an example of this, take the 1000 mA and 1500 mA LM-80 data and TM-21 projections developed for Cree's XLamp® XP-G LED (see **Table 1**).

We have provided three operating parameters that a few years ago would have seemed very aggressive in terms of drive current and operating temperature, but today fall within the bounds of a reliably designed system. At 1000 mA and 85°C $L_{70reported}$ is 51,400 hours and $L_{70reported}$ is 363,000 hours and At 1000 mA and 105°C $L_{70reported}$ is likewise 51,400 hours and $L_{70reported}$ is 105,000 hours. Even at Max Current for XP-G 1500 mA and an operating temperature of 85°C $L_{70reported}$ is still 51,400 hours and $L_{70reported}$ is 163,000 hours over 18 years of continuous operation[2] (see **Figure 2**)

Further, with 9,000-hour data sets, according to TM21 methodology, the XLamp XP-G LED, driven at 1000 mA, 85°C, $L_{95(9K)\ reported}$ is 42,300 hours and the reported $L_{90(9K)\ reported}$ is greater than 51,5400 hours. Color shift over time is similarly well behaved at higher currents and temperatures, with shifts of less than 0.004 d u'v' in all cases, and as shown in **Figure 3** below.

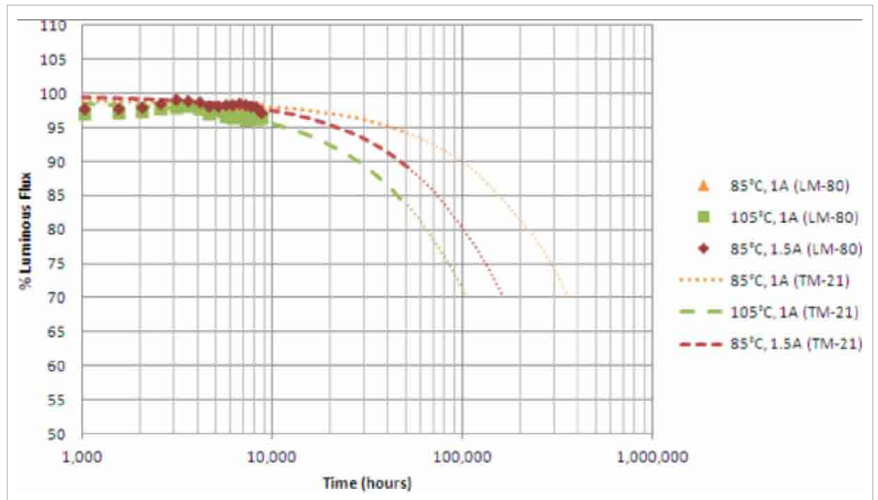

Figure 2: Graphical Representation of XLamp® XP-G LED TM-21 Reported L70 Projection at 1000 mA and 1500 mA

Similarly, at a maximum rated drive current of 2000 mA, the tabular data for XM-L LEDs, shows reported L70 projections of 61,000, 72,600 hours and 47,100 47,1000 hours, but also calculated projections from 306,000 hours (at 55°C) to 53,800 hours (at 105°C).

8000-plus hours of LM80 Color Shift data for the XLamp XM-L LEDs shows a d u'v' shift below 0.004 at 2000 mA and 55°, 85° and 105° C (see **Figure 4**). Based on this data, the XLamp XP-G

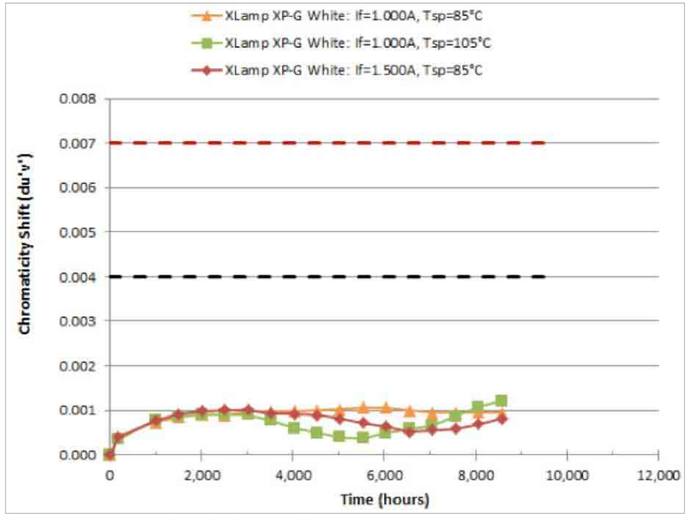

Figure 3: LM80 Color Shift Data for XP-G

and XM-L LEDs do not need to be driven at 350 mA, nor maintained at a low ambient temperature to achieve a long-lived, chromatically stable system designs.

LED systems design is always a series of tradeoff between power consumption and operating temperature. The LEDs themselves exhibit quasi-linear performance in a number of their operating parameters. *What's new in the progression of LED technology is that LEDs capable of higher current operations make the optimization of these non-linearities (droop, hot-cold factor and all the rest) a substantially less pressing design concern.*

For example, Cree's brightest cool white, single-die LED components evaluated with Cree's Product Characterization Tool (see **Figure 5**) shows us at a "reasonable" operating temperature of 55° C, the

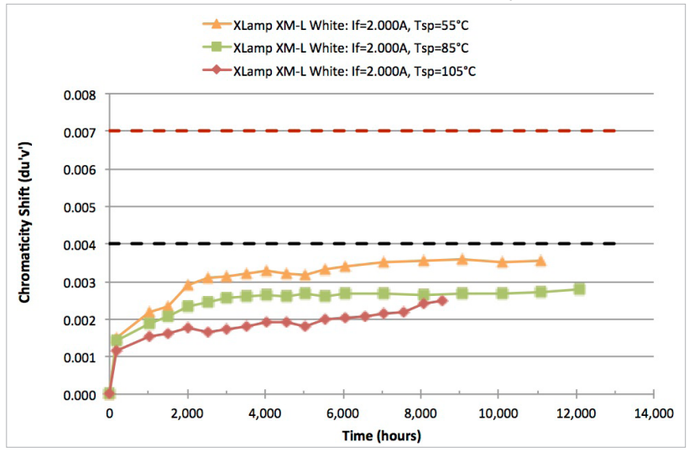

Figure 4: 9K Hours of LM80 Color Shift Data for XM-L

LEDs are all capable of delivering component efficiencies **well above 100 lumens/Watt at elevated drive currents.**[3]

Similarly, even with warmer phosphor mixtures, Cree's brightest warm white, single-die LED components deliver 75-90 lumens/Watt at 55°C, at drive currents well above the binning current.

LED component manufacturers, who provide engineering tools to perform system analyses, allow for rapid, basic performance assessment. *When long-term performance and reliability data are available over a wide range of operating conditions, device and component-level non-linearities need not be important selection criteria*. They are simply attributes of the devices to be taken into consideration during the design cycle. Long-term performance data at elevated current and temperatures allows an assessment of whether there is a valid concern for a particular manufacturer's particular LED component under consideration.

Driving LEDs at higher drive currents and/or elevated temperatures allows the designer to extract more lumens from each LED, use fewer LEDs, and fewer ancillary components. This in turn allows for lower system cost. There are practical constraints, of course as the following examples illustrate.

Current (A)	LED 1				LED 2				LED 3			
	Model: Cree XLamp XM-L2 (BWT)				Model: Cree XLamp XP-G2 (BWT)				Model: Cree XLamp XT-E (AWT)			
	Flux: U2 [300]			300.0	Flux: R5 [139]			139.0	Flux: R5 [139]			139.0
	Price: $ -	Tj (°C)		55	Price: $ -	Tj (°C)		55	Price: $ -	Tj (°C)		55
	ΔVf: 0.000	Multiple		x1	ΔVf: 0.000	Multiple		x1	ΔVf: 0.000	Multiple		x1
	LED lm	LED lm/W	LED Vf	LED W	LED lm	LED lm/W	LED Vf	LED W	LED lm	LED lm/W	LED Vf	LED W
0.350	167.9	171.7	2.79	0.978	148.3	148.5	2.85	0.999	149.3	145.8	2.93	1.024
0.400	190.7	169.6	2.81	1.124	167.3	145.3	2.88	1.151	167.6	141.7	2.96	1.183
0.500	235.3	165.7	2.84	1.42	203.8	139.4	2.92	1.462	202.5	134.2	3.02	1.509
0.600	278.7	161.8	2.87	1.722	238.3	133.9	2.97	1.78	235.1	127.5	3.07	1.844
0.700	320.8	158.1	2.9	2.029	271.2	128.9	3.01	2.104	265.7	121.6	3.12	2.186
0.800	361.8	154.6	2.93	2.34	302.4	124.3	3.04	2.433	294.5	116.2	3.17	2.535
0.900	401.7	151.3	2.95	2.656	332.2	120.1	3.07	2.766	321.7	111.3	3.21	2.89
1.000	440.5	148	2.98	2.977	360.8	116.3	3.1	3.102	347.3	106.8	3.25	3.252
1.100	478.3	144.9	3	3.301	388.1	112.8	3.13	3.44	371.7	102.7	3.29	3.62
1.200	515.1	141.9	3.02	3.63	414.5	109.7	3.15	3.779	394.9	98.8	3.33	3.996
1.300	550.9	139	3.05	3.962	440	106.8	3.17	4.119	417.2	95.3	3.37	4.379
1.400	585.8	136.3	3.07	4.298	464.8	104.3	3.18	4.457	438.8	92	3.41	4.771
1.500	619.8	133.7	3.09	4.637	489.1	102	3.2	4.793	459.9	88.9	3.45	5.174
1.600	653	131.2	3.11	4.979								
1.700	685.5	128.7	3.13	5.325								
1.800	717.1	126.4	3.15	5.674								
1.900	748.1	124.1	3.17	6.026								
2.000	778.4	122	3.19	6.381								
2.200	837.2	117.9	3.23	7.102								
2.400	893.9	114.1	3.27	7.836								
2.600	948.8	110.5	3.3	8.585								

Figure 5: 55° C Data for cool white XLamp® XM-L2, XP-G2 and XT-E LEDs

Cree's XLamp MT-G EasyWhite® LED is a multi-die LED, optimized for high-output, small form, directional lighting applications. The maximum current rating for the MT-G is 4000 mA, a substantial 24 Watts in a 9X9 mm package. But a small form bulb, such as a MR-16 cannot dissipate 20+ watts of thermal load. Based on Cree's experience in building a MR-16 reference design[4] we found heat sinks for the MR-class illumination sources could safely dissipate 4-7 watts of power (see **Figure 6**). The geometry of the heat sink constrains the drive capacity of the LED system. The MT-G LED, when used in a larger heat sink – such as a heat sink to support a PAR38 bulb application with several times the mass of the MR-16 heat sink– can support a much higher current (see **Figure 7**).

Cree's Shenzhen Technology Center developed examples of LED operating capacity, building two 6-inch recessed downlight fixtures using Cree's XLamp XP-G LED. Using the same mechanical enclosure and heatsink, but with different drivers and number of LEDs, we show output, distribution, CCT and CRI. One design uses 12 XP-G LEDs being driven at the LED's 350 mA binning current; the other uses 5 XP-G LEDs driven at 1000 mA.

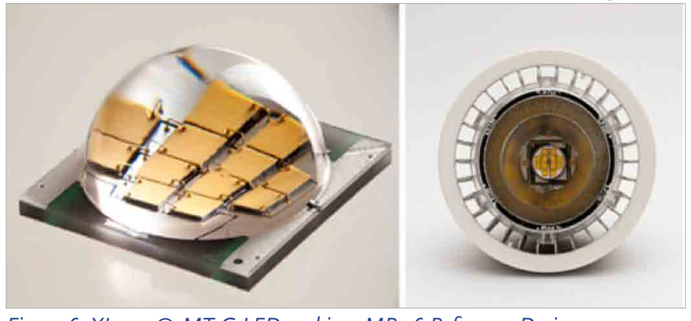

Figure 6: XLamp® MT-G LED and in a MR-16 Reference Design

Though differing in efficacy, both downlights deliver the efficacy, correlated color temperature (CCT) and color rendering index (CRI) required to meet ENERGY STAR® performance levels[5].

In this example one can reduce the number of LEDs in a fixture by 60%, obtaining almost identical optical performance in exchange

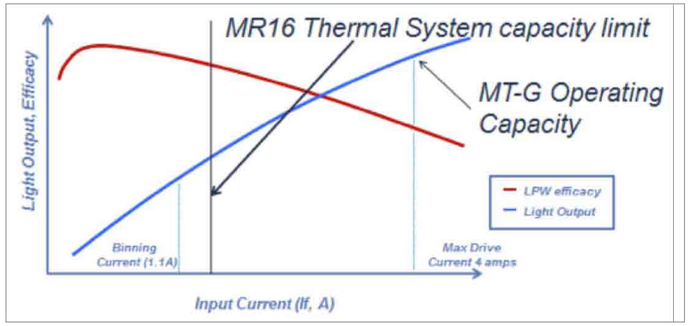

Figure 7: Visualizing the System Limits of a MR-16 Bulb Application

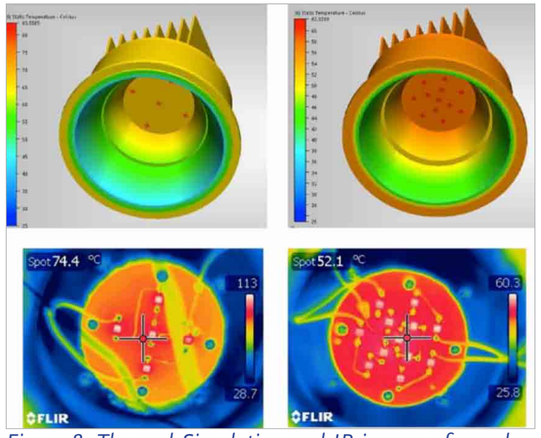

Figure 8: Thermal Simulation and IR images of 5 and 12 LED 6" Downlights

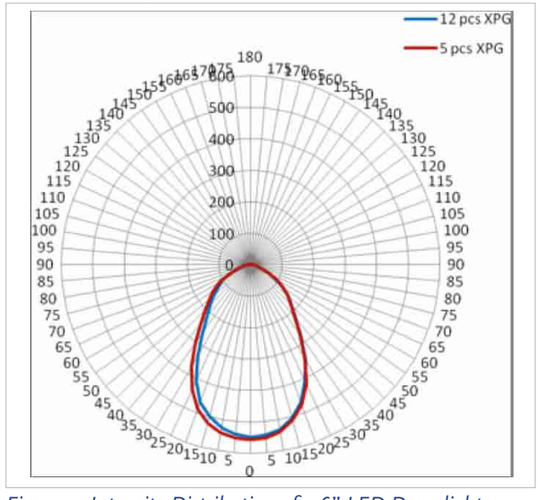

Figure 9: Intensity Distribution of 2 6" LED Downlights

for an elevated, but still reasonable operating temperature and reduction in system efficacy (see **Figures 8 and 9**).

LEDs have far more luminous capacity than most designers are using. The highest quality LEDs are capable of operating at sustained, elevated currents far above manufacturers' binning information so long as they do not exceed the manufacturers' specified maximum current. New luminaire and lamp designs should take advantage of these attributes. For lighting class LEDs, there is no reliability penalty for using more of this capacity. So what are you waiting for?

References

1. IES TM-21-2011, "Projecting Long Term Lumen Maintenance of LED Light Sources," now available at www.ies.org, recommends a method of projecting LED lumen maintenance, based on LM-80-08 data. The recommendation provides for 1) extrapolating LM-80 data sets to estimate a Lxx lifetime, where xx can be 70,80, 90,... 2) interpolating operating temperature lifetime from matched data sets, and 3) allows for calculated (extrapolated) and reported (6X LM-80 data sets) lifetime.
2. Calculated L70 values are for informational purposes only and are not a warranty or specification
3. These flux bins are current as of summer, 2013.
4. For additional details see, Cree XLamp LED Operating Capacity and XP-G 6-inch Downlight Reference Design, Cree Application Note CLD-AP89
5. ENERGY STAR® Program Requirements, Product Specification for Luminaires (Light Fixtures), Eligibility Criteria, Version 1.1

www.cree.com

Special Report: Automotive

PSD EUROPE

Power Systems Design: Empowering Global Innovation

Inside:

Circuit protection technology overview for automotive applications

Electronic equipment and systems have replaced many mechanical devices in automotive systems

By: Kelly Casey, Mouser Electronics

Automobiles produced today have a longer life expectancy than at any time in the past. This is due, in part, to improvements in materials and design. One critical change has been the increase in electronic equipment and systems that have replaced mechanical devices. Without proper electrical protection, however, these electronic systems can fail without warning, leaving the consumer to wish for the "good ol' days".

Designing electronics for the automotive environment is very challenging. Wide temperature swings must be anticipated. Most applications require the industrial temperature range of –40° to +85°C. Under-hood applications can be even more extreme. Humidity can range from desert lows to swamp highs. Add in seaside salt mist, road salt, or just lots of time; and corrosion can affect the quality of electrical connections and electrical insulation. Shock and vibration must be taken into consideration, along with the possibility of pinch points occurring where wiring is run throughout the vehicle where there is relative motion of doors, seats, windows, mirrors, pedals, steering columns, etc.

ESD Protection

Electrostatic discharge has several sources. A charge can build up on passengers as they move about the vehicle interior. The simple act of plugging in a personal device to the car's sound system can inject ESD into the system inputs. Dry air moving over a car antenna can cause ESD to build up on the radio inputs. Technicians working on electronic systems can inject ESD into ports not normally accessible by the car occupants.

Multi-Layer Varistor (MLV) devices are a classic ESD protection device. For example, the MLA series of MLVs from Littelfuse have capacitance values in the hundreds of pF, so they may not be appropriate for high-speed data lines. Polymer ESD devices such as TE Connectivity's PESD series offer capacitance below 1pF. High-performance low-capacitance ESD devices employ an encapsulated air gap. The CG0402MLU family of devices from Bourns is an example of this, with a maximum capacitance of just 0.05pF. All three of these technologies, however, have rather high instantaneous "let through" voltages that often exceed 100V during ESD events. To limit these voltages, one must use silicon diode technology such as Littelfuse's SP3021 series, which offer lower clamping voltages and low capacitances under 1pF. One drawback is that the silicon technology devices can cost ten times as much as the other technologies.

Load Dump Protection:

Load dump power surges are unique to automotive applications. Load dump pulses are momentary voltage spikes on the car's 12V power bus caused by the rather slow regulation of the alternator output voltage. The sudden removal of a large load on the power bus (such as a disconnected battery, a blown power fuse, etc.) will cause the alternator output to suddenly jump to 60 volts or more. It can take as long as 400 milliseconds for the voltage to recover to normal tolerances.

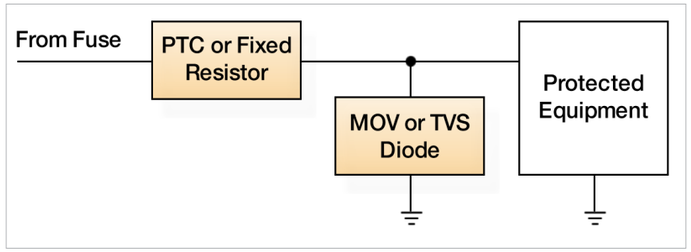

Figure 1

Compared to ESD pulses, which are measured in picoseconds, or lightning pulses, which are measured in microseconds, these load dump pulses are very, very long. TVS diodes have surge ratings measured with a pulse with a half-life of just one millisecond. This means that a typical 600W TVS diode may not survive even a 10W pulse that lasts 400 milliseconds. For a 15-volt diode, that's less than one amp! Fortunately, many alternators include surge suppression diodes that can reduce the load dump protection requirements of equipment installed in the car. Solutions for load dump requirements may include metal oxide varistor (MOV) or transient voltage suppressor (TVS) diode devices as overvoltage protection coupled with fixed resistors or positive temperature coefficient (PTC) resistors used to limit the surge current (see **Figure 1**).

One must be very careful in selecting components as the datasheets are geared toward much shorter surge pulses and extrapolating the surge withstand ratings to the load dump pulse range is tricky. Silicon overvoltage devices offer precise clamping voltages that assure the protected circuit will survive.

Short Circuits (Application Loads) and Power Faults:

The factory-installed fuses and circuit breakers handle short circuits in the power distribution wiring of an automobile. However, short circuits and other faults can also occur in the wiring between controllers and their loads. Examples include window defrosters, door locks, auxiliary lighting, and trunk-mounted sound systems. Shorts can occur due to corrosion at critical connectors and at pinch points where intermittent grounding of conductors can occur.

Power faults can also occur due to voltage regulator failure, and reverse polarity may occur due to improper jump-start connections and wiring errors during installation. It is even possible to experience a power cross event due to a pinch point or corrosion where a power line injects full battery voltage onto a low voltage control line or delicate sensor input. Protection against reverse polarity is usually accomplished by a series diode on the power input. The diode must be rated to handle the current of the fuse feeding the protected equipment.

It is possible to design the equipment I/O ports to be "hardened" to withstand these events using active protection circuitry (current limiters, auto shutdown, etc.). Yet all too often the need for such protection is not realized until late in the design cycle. At that point the design flexibility is often limited to adding additional protection circuitry.

One-time fuses can be used to open under fault conditions – however, this only prevents further damage or a fire. Once the fuse is operated, the circuit will not be operational and the equipment must be repaired, or more likely, be replaced.

PTC devices act as automatically resetting fuses in many applications. At normal operating currents, a PTC has a low resistance value. However, when fault currents are present, the PTC device warms up, increasing its resistance and pinching off the fault current. When the power or the fault is removed so that the PTC

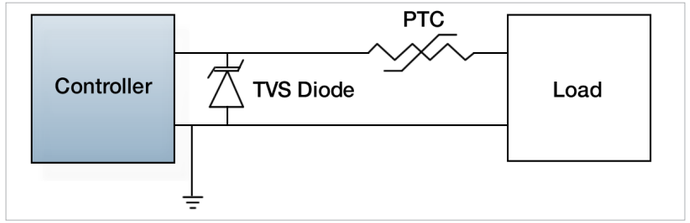

Figure 2

is allowed to cool to its original temperature, it will reset to its normal low resistance. To avoid nuisance tripping, one should be careful to select PTC devices with an extended temperature range. Devices such as the Bourns MF-RHT Series have a maximum operating temperature of up to 125°C, well above the normal PTC maximum operating temperature of 85°C. Designers should also note that at very low ambient temperatures, PTC devices might take a very long time to trip. Fortunately, the driving circuitry also has substantial thermal margin in these situations.

To protect against power cross events, TVS diodes are typically deployed to clamp the voltage on control lines and sensor inputs. For prolonged overvoltage events, current limiting must be included to prevent the TVS diode from overheating. **Figure 2** shows a typical I/O line where the TVS diode provides the overvoltage protection and the PTC provides both shorted load protection and power cross current limiting.

Whatever your circuit protection requirements might be, make sure to think about it early on in the design process. Mouser.com is a good place to find what you need, and they break packs if you are manufacturing a low-volume prototype run.

www.mouser.com

High-accuracy current measurement in automotive applications

New technology provides measurement and control options

By: Ramon Portas & Gauthier Plagne, LEM

The automotive industry has been undergoing a major transformation during the past few years. After more than a century of improving and refining the traditional gasoline and diesel engines that power automobiles, car manufacturers are now increasingly supplementing this traditional technology with some form of electrical boost. These so-called "hybrid" vehicles are capable of meeting or exceeding customer expectations in terms of power and response whilst consuming less fuel and hence emitting fewer exhaust gases.

The new electrical systems in these vehicles, including braking energy recovery systems, start-stop capabilities and electric motors driving the wheels, all require accurate measurement and control of the electricity flowing in the vehicle to optimize their performance and avoid a catastrophic failure. An essential part of these systems is the battery current sensor that measures the battery's charge and discharge level, and its state of health. There are several existing technologies for making a good automotive battery current sensor. The shunt has been the choice of some car manufacturers, while others prefer to use Hall-effect or fluxgate sensors in their designs. As with most things, each technology has its advantages and its drawbacks.

Shunt-based sensing

Shunt-based current sensors have been used widely in the last decade to measure battery currents (predominantly in premium-segment cars). These cars employ advanced electronics to accurately track the battery's charging capacity and overall health, and sometimes some form of performance-enhancing electrical assistance. The shunt is a resistor made of relatively expensive materials such as Manganese or Nickel-Chrome alloys, whose impedance is very low, well known, and precisely characterized over a range of temperatures and voltages. By measuring the voltage drop across the shunt resistor, the current flow through the resistor can be calculated using Ohm's Law.

This resistor is placed in the path of current flow to and from the car's battery, providing accurate, high-resolution information about the voltage and current (a temperature sensing feature is also added). Additionally, they can measure a very wide range of current amplitudes, from milliamperes to over one thousand amperes in short bursts (experienced when the car starts). Shunts do have a problem when measuring very high currents, as they must be proportioned to accept the high current flows, and they also dissipate significant power. These advantages and the absence of equivalent-performance alternatives over the past decade have made them a preferred choice for premium-market car makers, albeit at a relatively high unit cost.

Hall-effect sensing

Hall-effect-based current sensors have been around in industrial applications for several decades, and have also in the automotive industry for many years as well.

I Accuracy - 0/60°C	Fluxgate CAB300-C SP2	Hall transducer DHAB S/44	Smart Shunt
Global error at 0A	+/-10 mA	+/- 250 mA	+/-30 mA
Global error at 20A	+/- 40 mA	+/- 800 mA	+/-70 mA
Global error at 300A	+/- 1000 mA	+/- 9000 mA	+/- 700 mA

Figure 1: Transducer accuracy

Hall-effect sensors are sensitive to magnetic fields. By concentrating the magnetic fields generated by the currents passing in the battery cable on the sensor's Hall-cell, for example, the sensor will output a signal that is proportional to the passing current. This signal can then be further processed in the analog or digital domain to eliminate noise, and to compensate for the errors inherent to the technology. An analog voltage output, or some form of PWM, or SENT signal output can then be provided to the vehicle's battery management processors, which, in turn will integrate it to determine the charge and/or battery health.

One of the characteristics of Hall-effect sensors that have prevented some carmakers, especially premium-market ones, from using them in their battery-management systems is their offset error. The electrical- and magnetic-offset errors increase the uncertainty of the measured signal. They cannot be fully compensated and can thus affect the calculations of battery-charge levels. Offset error is also temperature dependent, sometimes with significant part-to-part variations. Shunt-based sensors lack these magnetic hysteresis effects. Overall errors of 3% to 5% were common in Hall-cell sensors of only a few years ago. The latest technological improvements reduce this error from 1% to 2% in many cases. Chip- and magnetic-core designs incorporating Hall-effect sensors are the main drivers of this improvement. (As a comparison, shunts have an accuracy of about %.)

Hall-effect sensors have several advantages over shunt-based sensors, the biggest ones being isolation and reliability. Hall-effect sensors are galvanically isolated from the primary current since they are placed near their target, and capture magnetic field information through space to create a reading. In this application Hall-effect sensor ICs are placed around the cable. They can also withstand much higher current and voltage peaks than other subsystems without sustaining damage. Since placement of Hall-effect sensors is not limited to the battery terminal post (as it is for most shunts); they can be placed anywhere along the cable or conductor whose current needs to be measured. This provides car manufacturers with significant economic benefits because they can source a single, standard component for use in any and all different engine and battery configurations with different cable lengths.

Hall-effect sensors are also generally much less costly to manufacture than equivalent shunts. Shunts employ high quantities of expensive materials and electronics to filter and condition the output signal, whereas Hall-effect sensors only require modest amounts of ferrous material and an integrated circuit (ASIC). If a shunt needs to provide a galvanically-isolated output, considerable additional cost needs to be added to the product. The compelling cost-benefit of Hall-effect technology has made many car manufacturers choose this technology for their battery current sensing applications, in exchange for modest reduction in accuracy, as compared to shunt-based alternatives.

Fluxgate technology

Fluxgate technology bridges the gap between Hall-effect sensors and shunts by providing the advantages of an isolated sensor with negligible signal-offset. For many years this has been a technology used in expensive industrial components, but fluxgate current sensors are now available in automotive-qualified solutions at comparable costs to the shunt. Much like Hall-effect sensors, they are sensitive to the magnetic fields generated around the primary cable, but their measurement principle is unique, and any signal offset is automatically cancelled

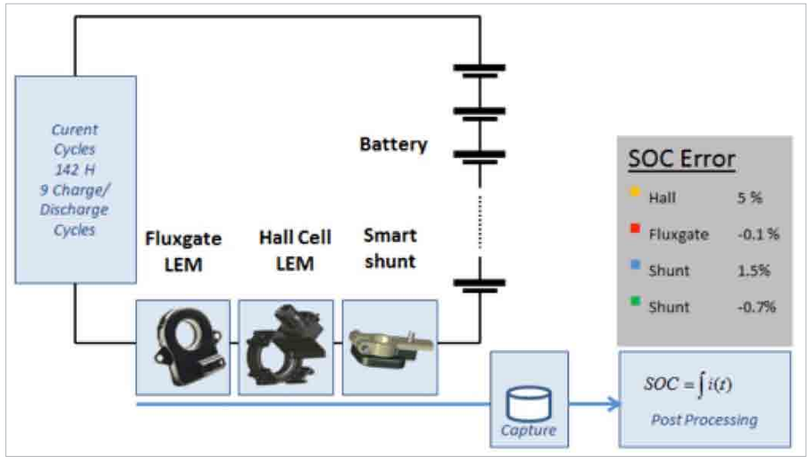

Figure 2: Current sensor comparison on SOC application

by the alternating currents in the windings of the solid magnetic core.

A fluxgate sensor's measurement error is less than 0.5% with a global offset lower than 10 mA in a 400 A-range product, giving them an inherent advantage (see **Figure 1**). When integrating current values over time to obtain the state-of-charge calculation in a vehicle, for example, the impact of the improved accuracy is multiplied, giving fluxgate sensors a clear advantage over Hall-effect, and even shunt-based technologies (see **Figures 2 and 3**). They can be also placed anywhere along the conductor, close to or far away from the battery, and thus offer flexibility of design to car manufacturers that helps them reduce costs. Fluxgate sensors are ideal for hybrid- and electric-vehicles where accurate current measurement is critical, and where the high-current amplitudes and sensor isolation pose a challenge to shunt-based alternatives.

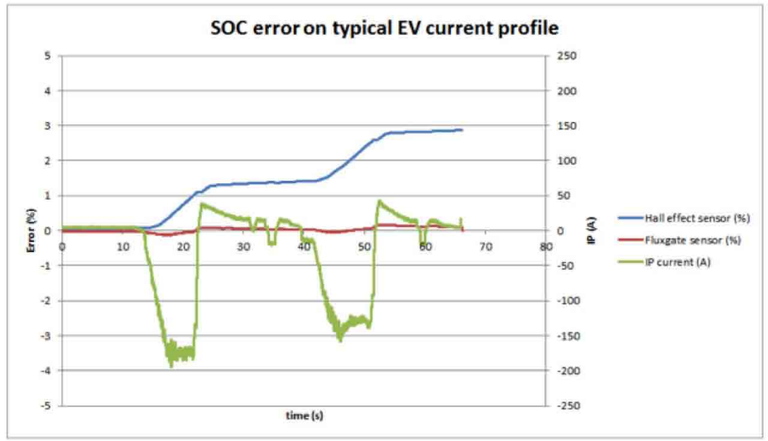

Figure 3: SOC error on typical EV current profile

Several technologies exist for measuring automotive battery currents, each with particular advantages and disadvantages. Premium-segment car makers have hitherto preferred shunt-based solutions due to their high accuracy and wide measurement range. Fluxgate technology, once reserved for very high-end industrial applications, has now been re-engineered to become price-competitive for automotive applications, and offers better accuracy than shunts whilst remaining galvanically isolated. When cost remains the biggest priority, Hall-effect sensors are the ideal solution. Their main historical drawback (offset errors) is being addressed with technological advances to provide accuracy in a/ low-cost product. The increasing need for electrical current measurements in cars gives an opportunity for these various technologies to further develop and become an essential element in the design and production of future automotive systems.

www.lem.com

Implementing multi-dimensional hall-effect sensors in automotive power steering

Magnetic-field sensor ICs are now in a plethora of different control mechanisms

By: Peter Riendeau, Melexis

Advances in automotive electronics are now leading to more widespread implementation of sensor ICs for the detection of magnetic fields. Devices of this kind are required for inclusion in a plethora of different control mechanisms found within modern vehicles. These include electric windows, electronic throttle, air conditioning, headlight positioning, electronic stability control (ESC), anti-lock brake systems (ABS), headrest positioning and engine management systems. One of their most important uses, however, is in electric power steering (EPS) systems (see **Figure 1**)

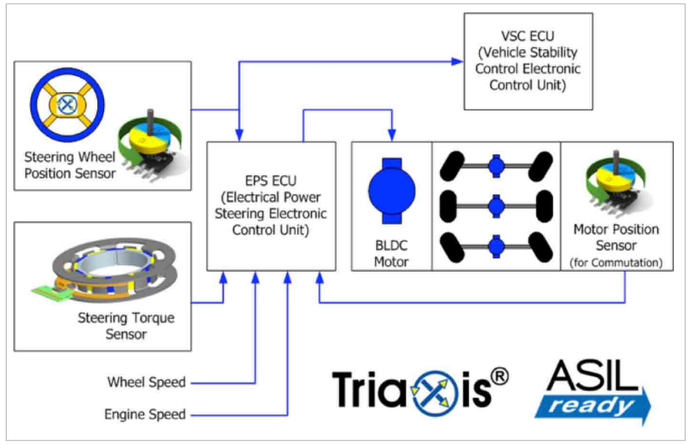

Figure 1: Typical EPS system with multiple sensors providing data to the ECU

EPS has advanced dramatically, supplanting traditional hydraulic power assist systems. Hydraulic systems were for decades the only method available for providing torque assistance and easing the effort required by the driver under low speed and parking situations. A hydraulic system consists of a vane rotor pump run from the accessory belt drive connected to the crankshaft of the engine. The continuous load of the pump can consume from 10-15% of the engine's power, whether there is steering torque assist needed or not. With the trend toward lowering emissions and increasing fuel efficiency, removal of this load presents a major opportunity to make improvements.

EPS not only eliminates the continuous load of a hydraulic pump, but also takes away the weight of the pump, its associated hoses and fluid reservoir from the overall weight of the vehicle. In addition, the removal of the hydraulic fluid along with its maintenance and disposal issues will have environmental benefits. EPS also supports the hybrid and electric vehicle trends as well as engine start-stop systems. An electric/hybrid vehicle has no moving parts in its engine when the vehicle is at rest and therefore a hydraulic power assist would not function when needed most, at low speeds and during parking maneuvers.

Inside an EPS system, magnetic sensor devices can provide the information needed for control of the mechanical torque boost, which will assist the driver with steering while the vehicle is travelling at low speeds or during parking procedures. Detection of a magnetic field and determination of its field strength (B) can be achieved using the Hall effect. This well established principle of physics describes the interaction of magnetic fields with current flow in a material. An accumulation of electrical charge resulting from this interaction will create a measurable voltage that relates proportionally to the size of the magnetic field present. Applying this principle to sensors enables many data concerning variations in position, proximity and speed to be acquired without contact being necessary and with high immunity to dirt, dust, vibration and temperature – highly suitable sensor characteristics for an automotive environment.
The basic elements of an EPS system are shown in **Figure 1**. Typically three different sensing mechanisms are required. These are: the steering torque sensor - which translates the torque applied by the driver to the steering wheel into an electrical signal for processing, the steering wheel position sensor - which provides the absolute position of the wheel, and the motor position sensor - which controls the commutation of the brushless DC motors.

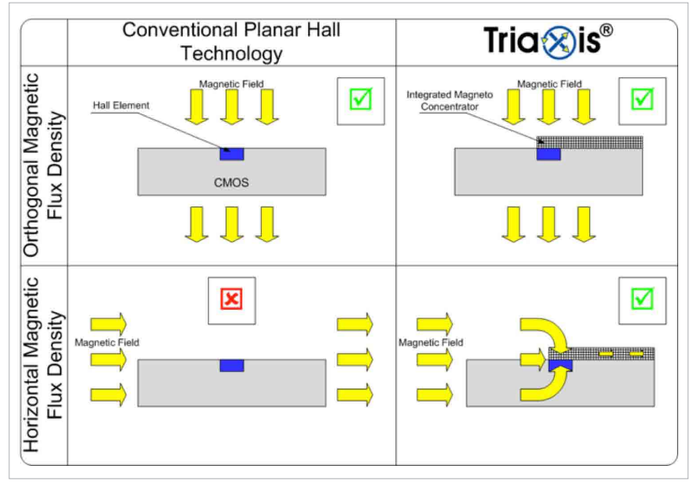

Figure 2: Conventional Planar Hall vs. Triaxis® Sensor Hall Sensing Elements with IMC® Film

An electronic control unit (ECU) processes the data that is output by these three sensors. It also receives data on the vehicle's speed and the rate at which the engine is running. The issue with employing conventional planar Hall effect sensors in automotive EPS systems is that they can only detect the magnetic field that is perpendicular to the sensor's surface. The control of such a system will therefore call for multiple planar sensors arranged perpendicular to one another. This has a number of operational disadvantages - namely increased component count, excessive bill of materials cost, a large amount of board real estate needing to be allocated and in many cases a long development process.

Multi-dimensional Hall Effect sensors

Several different multi-dimensional sensing solutions have been introduced on to the market in recent years. The Hall-based solutions mainly utilize the emerging Vertical Hall technology. Although it relies on the same basic principle, this integrated technology is still at the early stage of the learning curve compared to the conventional Planar Hall technology used in sensor ICs for more than 30 years. Using its own innovative proprietary technology, Melexis has developed a family of next generation multi-dimension Hall effect sensors in small form factor packages, which combine high performance characteristics

with rugged construction and highly cost-effective manufacture.

These Triaxis® devices have two pairs of orthogonal sensor elements running in both directions along the surface of a mixed signal CMOS chip. The patented IMC® (Integrated Magnetic Concentrator) film, made from ferromagnetic material, is subsequently deposited onto the chip. It enables the magnetic field around the IC to be shaped and enhanced, so that sensitivity can be increased and noise levels lowered. Using this in conjunction with specially created algorithms, it is possible for the magnetic flux components that are horizontal to the chip (BX and BY) to be quickly and accurately ascertained, in addition to the flux that is vertical to it (BZ). In **Figure 2** a comparison between conventional Planar Hall Effect sensors and Triaxis devices is made – showing how both horizontal and orthogonal flux can be addressed by the latter.

Through utilization of this technology, the quality of the BX and BY measurement signals will be fully in line with that from the BZ sensing element so that all three magnetic field components can be determined with equal accuracy. As a result, superior data on rotational or three-dimensional displacement can be acquired (with ±1° accuracy on a 360° rotation). All three of the differential voltages acquired by the sensor are then applied to an integrated ADC for conditioning. On-chip digital signal processing is then applied, in order to give a precise absolute position measurement. In an EPS system this means that the sensor can encode a mechanical angle into two sinusoidal voltage signals with 90° phase shift. The two voltage signals, which are proportional to the BX and BY magnetic field components, are then amplified and converted into digital form, with angular information being determined from application of an algorithm to the ratio of VX/VY.

EPS can contribute significantly to energy savings by eliminating the parasitic power losses of the hydraulic pump found in conventional steering assist systems. As a result the engine experiences less torque load, or it is possible that a smaller displacement engine might be used in the same vehicle. The power assist required for parking or low speed manoeuvres would be managed with stored energy from the existing battery. Multi-dimensional sensor technology has a key role to play in the deployment of more effective EPS systems. By creating such intricate sensor structures, where several sensing elements are integrated into a single semiconductor die, precise data on the various constituent steering components of an EPS system can be delivered. This enables the exact position of a vehicle's steering wheel to be derived, thereby enhancing EPS system performance and increasing the degree of safety that can be achieved.

Sensing solutions, such as the ones now available from Melexis, can not only mitigate the board level design issues inherent in systems made up of several discrete sensors, but also offer a simpler and more convenient way to implement multi-dimensional sensing than alternative solutions currently offered. Other uses for multidimensional sensors are found in power train applications including transmission position and shift-by-wire solutions. Such advanced systems are helping reduce energy consumption with highly refined "robotized" manual transmissions. In such case a conventional or even dual clutch standard shift transmission with its inherent mechanical efficiencies can be made to operate under complete electronic control with optimized shift points, maximizing fuel economy. These new sensors reach all of the necessary performance benchmarks and hit the desired price points too.

www.melexis.com

Power MOSFETs for automotive applications now come in smaller packages

More compact devices are required to address industry demands

By: Kieran McDonald, On Semiconductor

As demand for better fuel economy, increasingly sophisticated safety features, and more infotainment capabilities continues relentlessly, the demands for and on electronic systems in automobiles keeps increasing as well. Vehicle production, currently lead by China, is estimated to grow at close to 4% per year over the rest of this decade and the semiconductor content is projected to grow at more than twice that rate.

With the increased use of electronics in the vehicle comes the need to reduce the size (and cost) of electronic modules. This need is complicated by the fact that the power required by all of the electrical loads in a vehicle continues to increase. The current load is now more than 2.5kW in a conventional fuel powered vehicle, and much more than that on hybrid and pure electric vehicles. All of these market factors are driving demand for smaller power switch components, particularly Power MOSFETs, of which more than one hundred are typically used in today's automobiles.

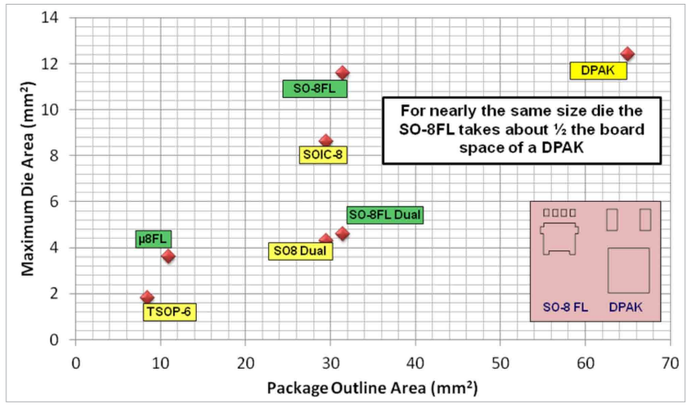

Figure 1: Die Area vs. Package Outline

Several years ago, the computer industry began switching to so-called 'flat lead' packages because they offered increased power density compared to traditional DPAKs for use in DC-DC converter power MOSFET output stages. (This was one of the enablers of thinner laptop PCs.) Several companies have taken these same packages, perhaps with a tweak or two, and qualified them to the stringent AEC-Q101 standards required by automotive electronics manufacturers.

ON Semiconductor calls these packages SO-8FL, SO-8FL dual, and µ8FL. The SO-8FL package dimensions are 5 mm x 6 mm x 1mm and the µ8FL package 3.3 mm x 3.3 mm x 1 mm. This compares to the DPAK whose dimensions are 9.9 mm x 6.5 mm x 2.3 mm. Despite the much smaller footprint of the SO-8FL package, it can accommodate a die that is nearly the same size as the maximum size die that fits in a DPAK. Reference the

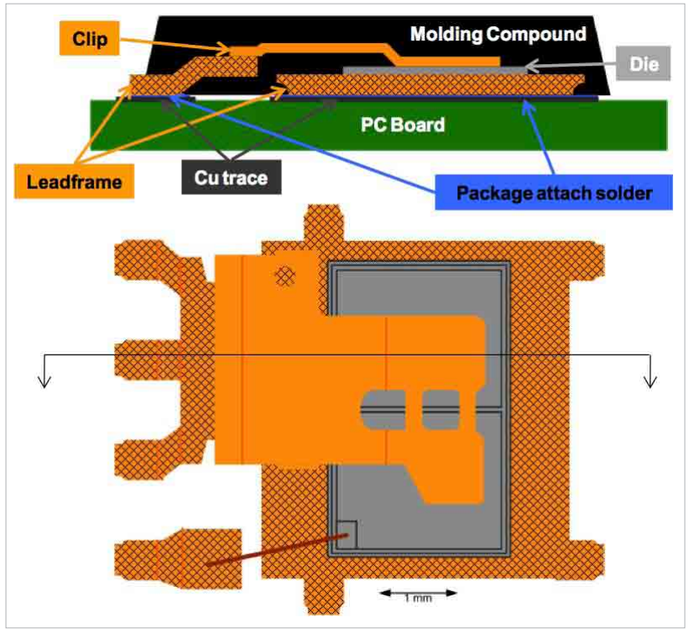

Figure 2: Top view and cross section of an SO-8FL package

diagram (**Figure 1**) below for a comparison of the footprint and maximum die sizes for the SO-8FL and µ8FL packages to other popular Power MOSFET packages.

Flat lead packages offer more than a size advantage over DPAKs. Their construction typically employs a copper clip to connect the source region of the silicon die to the pins on the package. This clip has a much lower resistance than the aluminum bond wires (even the two 20-mil-thick wires that can be used on the largest die) used in virtually all DPAK Power MOSFETs. This reduced resistance, as much as 0.7 mOhms, enables MOSFETs in SO-8FL packages to have lower on resistance than in DPAKs, even though the die is not larger. Products using the SO-8FL package are available today with $R_{DS(on)}$ values of less than 1 mOhm. The diagram below (**Figure 2**) shows the internal construction of an SO-8FL package with the clip connecting the source and a small diameter wire bond on the gate lead.

One concern engineers might have with these smaller packages is thermal resistance. Since thermal resistance from the package to the mounting board is primarily dependent on the size of the die, there is very little difference in the thermal resistance of a product with similar electrical specifications – breakdown voltage and $R_{DS(on)}$, assuming the same silicon technology is used for both the DPAK and the SO-8FL. A comparison of the transient thermal impedance of two products with the same die size, one using a DPAK and the other an SO-8FL package, is shown in the plot below (**Figure 3**)

The total system thermal impedance will be impacted by the manner in which the devices are mounted onto the PCB, the heat sinking used, airflow, and the heat dissipated by nearby devices. With the larger footprint of the DPAK package, there is the possibility to use a larger mounting pad, more thermal vias, and a larger heat sink, which would lower the overall thermal impedance for the device. However, the SO-8FL offers the ability to safely dissipate a lot of power in a much smaller footprint than is possible with a DPAK.

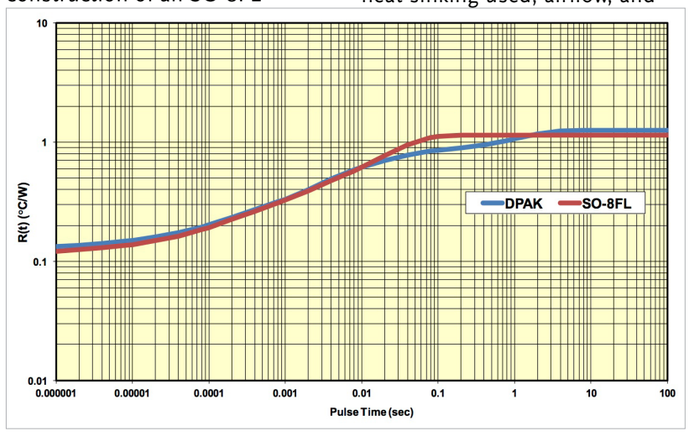

Figure 3. Transient thermal impedance, junction to mounting board

Another concern some manufacturing engineers have with these small packages is the ability of their automated optical inspection systems to see the solder joint to the PCB. The SO-8FL and µ8FL packages were designed so that the leads protrude from the plastic edge of the package by about 150 microns. The top, bottom and sides of these leads are tin plated for good solder wetting. This means a nice, visible meniscus is formed on the sides of the leads when the unit is soldered to the board. For AOI systems that cannot adequately see the sides of the leads, a 'wettable flank' option is available that adds tin plating to the tips of the leads. This has been shown to provide excellent visibility to AOI equipment that otherwise had some difficulty inspecting the solder joints.

Purchasing departments are always concerned about cost, so the question arises that since these are relatively new packages won't the cost be more than the very mature DPAKs? Due to the very high demand generated by the computer and wireless markets for these small packages, they have reached extremely high volumes, and costs are now at parity with the DPAK. With the cost savings that can be achieved by using smaller PCBs and modules derived from using flat lead packages, overall system costs will be reduced.

An ever-expanding portfolio of flat lead Power MOSFETs in single and dual SO-8FL packages and in the even smaller µ8FL package is available with AEC-Q101 qualification from ON Semiconductor and other suppliers. Products are available in voltages of 30, 40, 60, and 100 V. N-channel and some P-channel products are available. Also available now are Power Rectifiers in the same packages. These products are being designed in and used in engine control units, fuel injection drivers, seat motors, windshield motors, anti-lock braking systems, LED and HID lighting, infotainment systems, and many other automotive systems. Within a few years it is expected that flat lead packages will exceed the number of DPAKs used in automotive electronic systems.

www.onsemi.com

Online Video Highlights

By: Alix Paultre, Editorial Director, PSD

Here are highlights from PSD's video podcasts on power systems and design engineering from the APEC and PCIM exhibitions, each showing some of the latest technologies and products. You can either enter the URL listed into your browser, or use your smartphone or tablet with the provided QR code to watch immediately.

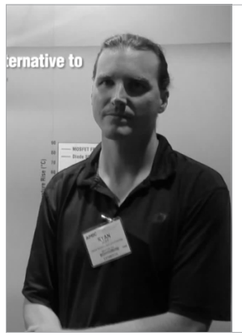

Linear

Linear Technology explains their FET bridge technology at APEC 2013

Ryan Huff, a Senior Applications Engineer at Linear Technology, explains their diode bridge controller technology at their booth at APEC 2013. Linear's approach replaces each of the four diodes in a full-wave bridge rectifier with low-loss N-channel MOSFETs to significantly reduce the power dissipation and increase available voltage.

http://tinyurl.com/PSD-Linear-APEC2013

Methode

Methode's SmartPower Stack embedded power technology at APEC 2013

SmartPower Stack™ is presented as the industry's first fully integrated, deployment-ready commercial embedded system for high volume solar, photovoltaic, wind, hybrid electric and electric vehicles, as well as high capacity uninterruptible power supply and efficient motor drive applications.

http://tinyurl.com/PSD-Methode-APEC2013

SBE

SBE explains their Bank Hardener capacitor technology at APEC 2013

Mike Brubaker, the CTO of SBE, a developer and manufacturer of film capacitors and systems, explains their Bank Hardener capacitor technology on the storage density of aluminum electrolytic capacitors, reducing by a factor of two of the number of AE cans, and an increase in AE bank life significantly.

http://tinyurl.com/PSD-SBE-APEC2013

LeCroy

Teledyne LeCroy demonstrates power analysis for efficiency at APEC 2013

At APEC 2013, Steve Murphy of Teledyne LeCroy demonstrates several of the company's latest devices for Power Systems Design and how they aid designers in power analysis for efficiency gains. Understanding phenomena like switching losses, conduction losses, and other power-robbing issues are critical to designing an efficient system.

http://tinyurl.com/PSD-LeCroy-APEC2013

Ridley Enginerring

Ray Ridley on Ridley Engineering's services at PCIM 2013

Focusing on power basics like magnetics, Ridley Engineering provides training & education on how to be a better power supply designer. Resources provided include books and tools to not only teach the engineer during the design course, but for long afterward as basic design tools and references for the job.

http://tinyurl.com/PSD-Ridley-APEC2013

International Rectifier

International Rectifier's latest COOLiR FET technology at PCIM 2013

Ben Jackson, the Senior Manager, Automotive Power Switch and Module Product Management at International Rectifier, explains their latest COOLiR™ FET-based automotive power switches. Targeting 40-V MOSFET applications, the devices have a low RDS(on) and high current capability.

http://tinyurl.com/PSD-IR-APEC2013

Amantys

Amantys' real-time "internet of things" using real trains at PCIM 2013

Richard Ord of Amantys shows their latest web-enabled cloud-driven IGBT drivers using ARM processors at PCIM 2013 for Power Systems Design. The demonstration involved real-time power monitoring and troubleshooting of an operating locomotive in the Portuguese rail system.

http://tinyurl.com/PSD-Amantys-APEC2013

Everyone needs to be an efficiency engineer now

By: Alix Paultre, Editorial Director, PSD

Once upon a time, to be an engineer who spent time trying to reduce power consumption meant you were either a power supply designer, or worked in the few application spaces that needed high-efficiency low-consumption systems (primarily military and aerospace).

Most people never thought about power consumption. Back then, the most prevalent issue then was delivery, with houses and factories having to add fatter and fatter lines to cope with the rising power consumption of the tools. Efficiency, if at all a consideration, was most commonly used to create a higher power output in the target product, not reduce overall consumption.

Things began to change decades ago, but have accelerated in an almost exponential fashion in recent years. In almost every market today, manufacturers are touting differences in efficiency of a several percent between them and a competitor as a significant product selling point. This is largely driven by our migration to portable devices, but also due to our desire to reduce excess consumption at the grid level as well.

The advantages to energy efficiency are many, and include longer operational life within a finite power budget (from a gas tank to a battery), more power output (more functionality) from a restricted power pipeline like USB or PoE, lower energy costs in any system (fixed or mobile) and reduced waste energy (usually expressed as heat).

The primary focus on energy management in devices today is battery management and device runtime, and that drives most product design. However, there is also a growing pool of products that are designed to be active peripherals, from external USB-driven speakers to interface devices to novelty items, each drawing power from the central unit. The limited power pipeline of hybrid power/signal interfaces like USB and Power over Ethernet is also an important factor to consider in device design.

It has gotten to where soon all of the passives around a device will designed specifically for that device family, to maximize system operating efficiencies and address the extremely tight performance tolerances these new ICs have. To truly achieve the phenomenal efficiency the latest chips are now promising, every single part, lead, trace, passive, and peripheral IC in the system must be the best possible for that specific circuit. Today, even package-level interconnect and mounting parasitics (the poster child for this is the TO-220 package) can significantly impact the operating efficiency of a device.

Another aspect of this is the continuing trend for more densely-populated SoCs and other highly-integrated devices to be more complete subsystems, reducing the need for any peripheral components at all in some systems. This integration will also increase as we move forward, and not only offer energy efficiencies, but also smaller and more robust devices. The biggest problem here is and will continue to be thermal management, as even a high-efficiency device has waste heat that must be dealt with.

www.powersystemsdesign.com

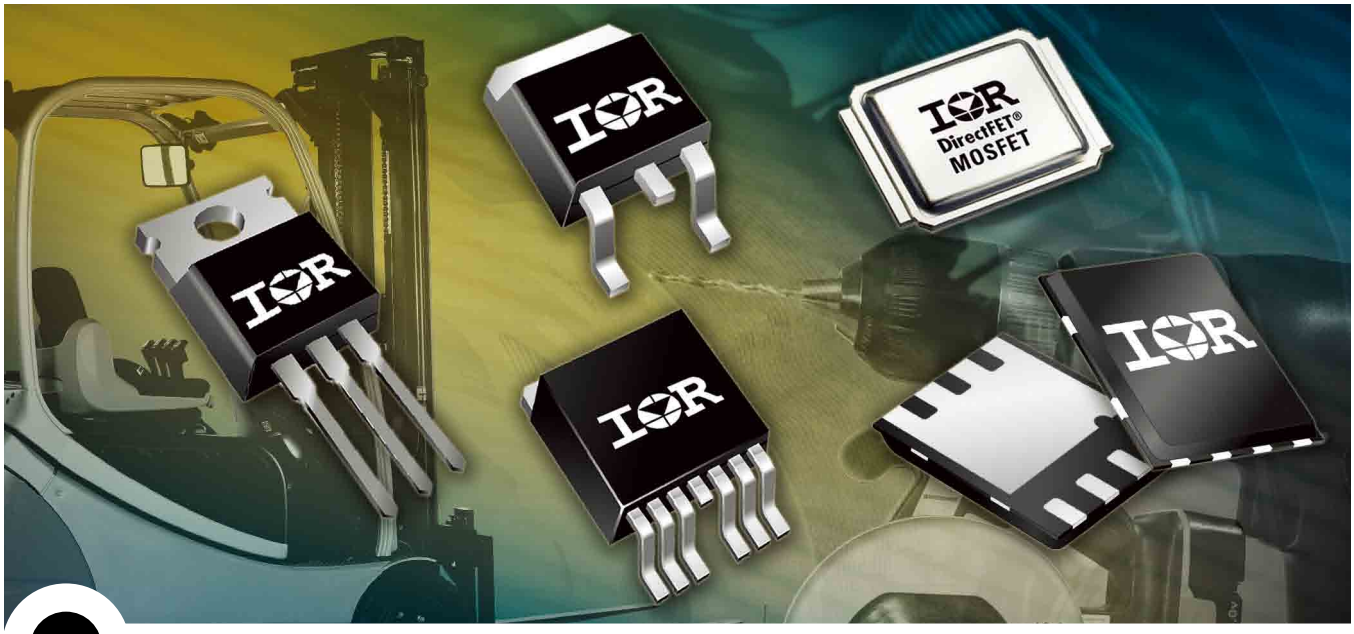

StrongIRFET™ Rugged, Reliable MOSFETs

Specifications

Part Number	B_{VDSS}	ID@ 25°C	$R_{DS(on)}$ max@ Vgs = 10V	Qg@ Vgs = 10V	Package
IRFH7004TRPbF	40 V	100 A	1.4 mΩ	134 nC	PQFN 5x6
IRFH7440TRPbF	40 V	85 A	2.4 mΩ	92 nC	PQFN 5x6
IRFH7446TRPbF	40 V	85 A	3.3 mΩ	65 nC	PQFN 5x6
IRF7946TRPbF	40 V	90 A	1.4 mΩ	141 nC	DirectFET Medium Can
IRFS7437TRLPbF	40 V	195 A	1.8 mΩ	150 nC	D^2-Pak
IRFS7440TRLPbF	40 V	120 A	2.8 mΩ	90 nC	D^2-Pak
IRFS7437TRL7PP	40 V	195 A	1.5 mΩ	150 nC	D^2-Pak 7pin
IRFR7440TRPbF	40 V	90 A	2.5 mΩ	89 nC	D-Pak
IRFB7430PbF	40 V	195 A	1.3 mΩ	300 nC	TO-220AB
IRFB7434PbF	40 V	195 A	1.6 mΩ	216 nC	TO-220AB
IRFB7437PbF	40 V	195 A	2 mΩ	150 nC	TO-220AB
IRFB7440PbF	40 V	120 A	2.5 mΩ	90 nC	TO-220AB
IRFB7446PbF	40 V	118 A	3.3 mΩ	62 nC	TO-220AB
IRFP7430PbF	40 V	195 A	1.3 mΩ	300 nC	TO-247

Features:

- Ultra low $R_{DS(on)}$
- High current capability
- Industrial qualified
- Broad portfolio offering

Applications:

- Battery Packs
- Inverters
- UPS
- Solar Inverter
- DC Motors
- ORing or Hotswap

For more information call +49 (0) 6102 884 311
or visit us at www.irf.com

International
IOR Rectifier
THE POWER MANAGEMENT LEADER